문서번호 APCC-출장-16-1454(2016-12-26)

TRAVEL REPORT FORM
출장보고서

결재	선임연구원	팀장	부서장	원장
	12/21 윤선권	12/22 조재필	12/26 김형진	12/26 정홍상
협조	팀장	부서장		
	12/22 김선태	12/26 유진호		

I. Reporter 보고자

Department 소속	Position 직위(직급)	Name 성명	Travel Date 날짜	Note 비고
기후연구팀	팀장	김선태	2016.12.11.-17	
〃	선임연구원	김무섭	〃	
응용사업팀	〃	음형일	2016.12.11.-18	
〃	〃	신용희	〃	
〃	〃	윤선권	〃	

II. Major Activities 주요업무 수행내용

1. Main Contents and Activities 주요내용 및 활동

□ 2016 AGU Fall Meeting
- 학회일정 : 2016.12.12.~2016.12.16. (5일간)
- 장 소 : 샌프란시스코, 캘리포니아 미국
- 출 장 자 : 총 5 인
  - 기후예측본부 : 기후연구팀(2인)-김선태 팀장, 김무섭 선임연구원
  - 응용사업본부 : 응용사업팀(3인)-음형일, 신용희, 윤선권 선임연구원

□ 2016 AGU Fall Meeting 학술발표, 연구동향 파악 및 연구내용 토론

AGU는 매년 전 세계 약 25,000명 이상의 연구자들이 참석하는 세계적인 학회로, 기초과학 및 응용과학 분야 최신 이슈들이 발표되었음. APCC 연구자들의 학술발표세션 및 내용은 다음과 같음

※ 학술발표세션 및 내용
- 김선태 팀장
  Session (A048): Tropical Pacific Ocean Mean Bias and ENSO Prediction Error
- 김무섭 선임연구원
  Session (GC032): Statistical downscaling of climate model prediction using weather generator: application to Korean Basin
- 음형일 선임연구원
  Session (GC055): Detection of changes in indicators of hydrologic alterations under CMIP5 projections from a model chain with a multi-model approach
- 신용희 선임연구원
  Session (EP036): Development of Soil Water Content Estimation Method on Agricultural Region

in South Korea

- 윤선권 선임연구원

  Session (H065) Seasonal prediction for hydro-meteorological variables in the Korean Peninsula: Links with atmospheric teleconnections

□ 한국인과학자 초청 세미나 및 간담회

재미 한국인 과학자 및 AGU참석 한국인 과학자를 초청하여 간담회 장을 마련하였으며, APCC 계절예측 자료 및 기후변화, 응용분야 연구에 대한 정보공유 및 인적네트워크를 구축하였음

※ 주요내용

- 목적: 재미한국인과학자 인적 Network 활성화 및 APCC 홍보
- 일시: 2016.12.13.(화) 11:00~14:00
- 장소: 888 Howard Street, San Francisco, CA 94103
  Intercontinental Hotel, SUTTER 홀(5층)
  (http://www.intercontinentalsanfrancisco.com/)
- 참석: 15인(AGU참석 한국인과학자 6인, POSTEC 2인, APCC임직원 6인, 기상청 1인)

2. Relevance to APEC Climate Center's Activities 결론 및 소감

▫ 기후과학 및 기후응용 분야 최근 현안 이슈, 연구동향 파악, 국제적 정책 동향 파악이 가능했음

▫ 수자원, 농업, 보건환경, 해안 분야 등 최근 현안 이슈에 대한 논의 및 인적 네트웍 구축

▫ Atmospheric Science, Global Environmental change, 그리고 Hydrology 분야에 APCC MME 예측 결과를 홍보할 수 있는 계기가 되었음

▫ 현재 기후 모델의 세계적인 개발 동향과 기후변화와 관련된 연구들에 활용되기 위한 노력들과 프로젝트에 대한 정보 공유하였으며, 기후 변화 관련 국제 프로젝트가 다양하며 APCC의 적극적인 기여가 바람직할 것으로 보임

▫ APCC의 계절예측정보에 대한 응용분야 활용이 점차 확대되고 있으며 향후 런천 참석자들의 연구 수행에 있어 필요한 기후예측 정보를 어떤 방식으로 제공하는 것이 바람직할지에 대한 논의가 이루어짐

▫ 재미한인과학자와 국내·외 관련 전문가를 한자리에서 만나 볼 수 있는 계기가 되었으며, APCC 홍보 및 국제적 네트웍 형성에 기여하였음

▫ 국외 응용분야 연구기관에서는 아직까지 APCC에 대해 잘 알지 못하고 있으나, 기후분야와의 융합연구의 필요성이 점차 강조 되고 있어 보다 적극적인 기관 홍보 및 인적 네트워크 구축이 필요하다고 판단됨

▫ 매년 열리는 AGU학회는 해외 거주 한국인 과학자들이 한 곳에 모이는 장소이며, 기후/응용 분야 인재 발굴 및 기관 홍보, 정보공유를 위한 네크워크 형성 장으로 활성화 필요할 것으로 판단되며, 향후, 지속적인 학회 참여와 간담회장 마련으로, 적극적이며 실효성 있는 성과 기대

III. References 참고사항

(with attachment of any information or report in case of attendance of conferences, workshops and meetings) 학술대회, 워크숍, 회의 등 참석 시 관련 정보 및 문서 첨부

1. Presented and Collected Materials 주요 수집자료

□ 2016 AGU Fall Meeting, Program Book

2. Suggestions and Remarks 건의사항

1. 김선태 박사

AGU FALL MEETING

San Francisco | 12–16 December 2016

A43D-0254: Tropical Pacific Ocean Mean Bias and ENSO Prediction Error

Thursday, 15 December 2016
13:40 - 18:00
Moscone South - Poster Hall

Utilizing Bjerknes coupled stability (BJ) index analysis, this study investigates a cause of errors in predicting the amplitude of the El Niño Southern Oscillation (ENSO)-driven sea surface temperature variability based on retrospective forecasts made with an APEC Climate Center seasonal forecast model. It is found that change in the ENSO amplitude from the hindcast simulations is represented well by change in the growth rate as estimated with the BJ index. We also find that the forecast errors in the ENSO amplitude are the most strongly associated with errors in both of the thermocline slope response and the surface wind response to a forcing over the tropical Pacific, leading to errors in the thermocline feedback. We conclude that an upper ocean temperature bias in the equatorial Pacific, which becomes stronger with increasing lead times, is a possible cause of forecast errors in the thermocline feedback and further ENSO amplitude.

Authors

Seon Tae Kim *
APEC Climate Center

Hye-In Jeong
APEC Climate Center

View Related Events

Session: A43D Dynamics, Observations, and Predictability in Light of the Recent 2015–2016 El Niño Event VI Posters

Program: Atmospheric Sciences

Day: Thursday, 15 December 2016

2. 김무섭 박사

AGU FALL MEETING

San Francisco | 12–16 December 2016

GC33A-1217: Statistical Downscaling of Seasonal Prediction using Weather Generator with Application to a Korea Basin

Wednesday, 14 December 2016
13:40 - 18:00
Moscone South - Poster Hall

GCM (General Circulation Model) is a basic and fundamental tool for predicting future climate conditions. Unfortunately, its output is too coarse in space and time to be directly applied to application fields. Currently, there is a large amount of research focused on closing the gap between resolutions of GCM output and application data. This process is called downscaling, for which many methods have been proposed in dynamical and statistical contexts. Statistical downscaling methods are frequently employed in hydrological and agricultural studies since it can rapidly downscale GCM output without expensive computational costs.

Among many statistical downscaling methods, weather generator is an attractive one producing climate data of daily time scale for a local region. However, most of weather generators are originally designed to simulate local weather based on climatology during observation period. Especially, inter-annual variability of climate is not taken into account. In this study, we develop a new weather generator linked with large-scale climate in order to reflect seasonal prediction into weather simulation. The basic idea is to parametrize local climate characteristics into the underlying weather generator model, then, to link it with large-scale climatic variables. It indicates that the values of parameters, representing the condition of local climate system, are varying according to that of large-scale climate.

We illustrate it by an application to a Korea basin. Local climate characteristics under consideration are monthly mean of daily maximum/minimum temperatures adjusted by precipitation effect, mean of dry-spell length, and precipitation intensity. The link between local and large-scale climate is quantified by regression model.

Author

Moosup Kim *
APEC Climate Center

View Related Events

Session: GC33A Environmental, Socioeconomic, and Climatic Changes in Northern Eurasia and Their Feedbacks to the Global Earth System and Society II Posters

Program: Global Environmental Change

Day: Wednesday, 14 December 2016

3. 음형일 박사

AGU FALL MEETING
San Francisco | 12–16 December 2016

Welcome, Hyung-Il Eum

Assigned Entries

To view the details of your presentation and accept or decline your participation at the 2016 AGU Fall Meeting, please click on the title below. Please accept or decline your participation by Thursday, 3 November 2016.

Time & Location	Session Title	Abstract Title	Role	Presentation Type
Monday, 12 December 2016: 13:40 - 18:00, Moscone South, Poster Hall	Quantitative Methods for Addressing Model Uncertainties in Climate and Hydrology Projections and Prioritizing Measurement Needs II Posters	Detection of changes in indicators of hydrologic alterations under CMIP5 projections from a model chain with a multi-model approach	Presenting Author	Poster

If you encounter any problems with this form, e-mail technical support.

4. 신용희 박사

AGU FALL MEETING

San Francisco | 12–16 December 2016

Welcome, Yonghee Shin

Assigned Entries

To view the details of your presentation and accept or decline your participation at the 2016 AGU Fall Meeting, please click on the title below. Please accept or decline your participation by Thursday, 3 November 2016.

Time & Location	Session Title	Abstract Title	Role	Presentation Type
Thursday, 15 December 2016: 08:00 - 12:20, Moscone South, Poster Hall	Soil State Characteristics: From Observations to Data Assimilation and Modeling I Posters	Validation of Soil Water Content Estimation Method on Agricultural Regions in South Korea	Presenting Author	Poster

If you encounter any problems with this form, e-mail technical support.

5. 윤선권 박사

AGU FALL MEETING

San Francisco | 12–16 December 2016

Welcome, Sunkwon Yoon

Assigned Entries

To view the details of your presentation and accept or decline your participation at the 2016 AGU Fall Meeting, please click on the title below. Please accept or decline your participation by Thursday, 3 November 2016.

Time & Location	Session Title	Abstract Title	Role	Presentation Type
Wednesday, 14 December 2016: 13:40 - 18:00, Moscone South, Poster Hall	Large-Scale Climate Variability and Its Impact on Hydrological Systems, Water Resources, and Population I Posters	Seasonal prediction for hydro-meteorological variables in the Korean Peninsula: Links with atmospheric teleconnections	Presenting Author	Poster

If you encounter any problems with this form, e-mail technical support.

A43D-0254

Mean Bias in Seasonal Forecast Model and ENSO Prediction Error

Seon Tae Kim (seontae.kim@apcc21.org) and Hye-In Jeong
APEC Climate Center, Busan, Korea

Abstract

This study uses retrospective forecasts made with an APEC Climate Center seasonal forecast model to investigate the cause of errors in predicting amplitude of El Niño Southern Oscillation (ENSO)-driven sea surface temperature variability. When utilizing Bjerknes coupled stability (BJ) index analysis, changes in ENSO amplitude from hindcast simulations are found to be well represented by the change in growth rate estimated by the BJ index. Forecast errors in ENSO amplitude are most strongly associated with errors in both the thermocline slope response and surface wind response to forcing over the tropical Pacific, leading to errors in thermocline feedback. This study concludes that upper ocean temperature bias in the equatorial Pacific, which becomes stronger with increasing lead times, is a possible cause of forecast errors in the thermocline feedback and further ENSO amplitude.

Hindcast Simulations

APCC CCSM3

- Atmosphere (CAM3, T85L26)-Ocean (POP1.4, 1° (1/3°)x1° , 40 Levels)-Land (CLM)-Sea Ice (CSIM4) coupled model

Wind-ocean temperature nudging initialization

- Simulated ocean temperatures and surface winds were strongly nudged toward their observations using a restoring time scale of five days and one hour, respectively, in a coupled mode

- Ensemble members : 5
- Ensemble generation methods: Time lagged forecasting method [Brankovic et al. 1990]
  - ✓ ATM/LSM/ICE ICs: last 5 days of each month
  - ✓ Ocean IC: 25th January, 24th February, 26th March, 25th April, 25th May, 24th June, 24th July, 23rd August, 22nd September, 27th October, 26th November, 26th December
  - ✓ Each simulation performs a **full 7-month integration** indicating forecasts from **0-month to 6-month lead times**.
- Hindcast period: 1982-2014 (33 years)

BJ index

Mean Advection Damping (MD) | Thermodynamic Damping (TD)

$$2BJ = -\left[\frac{\langle \Delta \bar{u}_E \rangle}{L_x} + \frac{\langle \Delta \bar{v}_E \rangle}{L_y}\right] - \alpha_s + \mu_a \beta_u \left\langle -\frac{\partial \bar{T}}{\partial x} \right\rangle_E + \mu_a \beta_w \left\langle -\frac{\partial \bar{T}}{\partial z} \right\rangle_E + \mu_a \beta_h \left\langle \frac{\bar{w}}{H_1} \right\rangle a_h - \varepsilon$$

Zonal Advective Feedback (ZA) | Ekman Feedback (EK) | Thermocline Feedback (TH)

$$\langle Q \rangle_E = -\alpha_s \langle T \rangle_E, \quad [\tau_x] = \mu_a \langle T \rangle_E, \quad \langle u \rangle_E = \beta_u [\tau_x] + \beta_{uh} \langle h \rangle_w$$
$$\langle H(\bar{w}) w \rangle_E = -\beta_w [\tau_x], \quad \langle h \rangle_E - \langle h \rangle_w = \beta_h [\tau_x], \quad \langle H(\bar{w}) T_{sub} \rangle_E = a_h \langle h \rangle_E,$$

- Describe **atmosphere-ocean coupled dynamics** in the tropical Pacific and estimate **overall linear ENSO stability** in a coupled system
- **Negative contributions** by **mean advection** and **thermal damping** and **positive contributions** by the **zonal advective, Ekman** and **thermocline feedbacks**
- Each positive feedback term as a function **of tropical Pacific Ocean mean state**, and **oceanic and atmospheric response sensitivity coefficients**

ENSO forecast errors in the APCC CCSM3

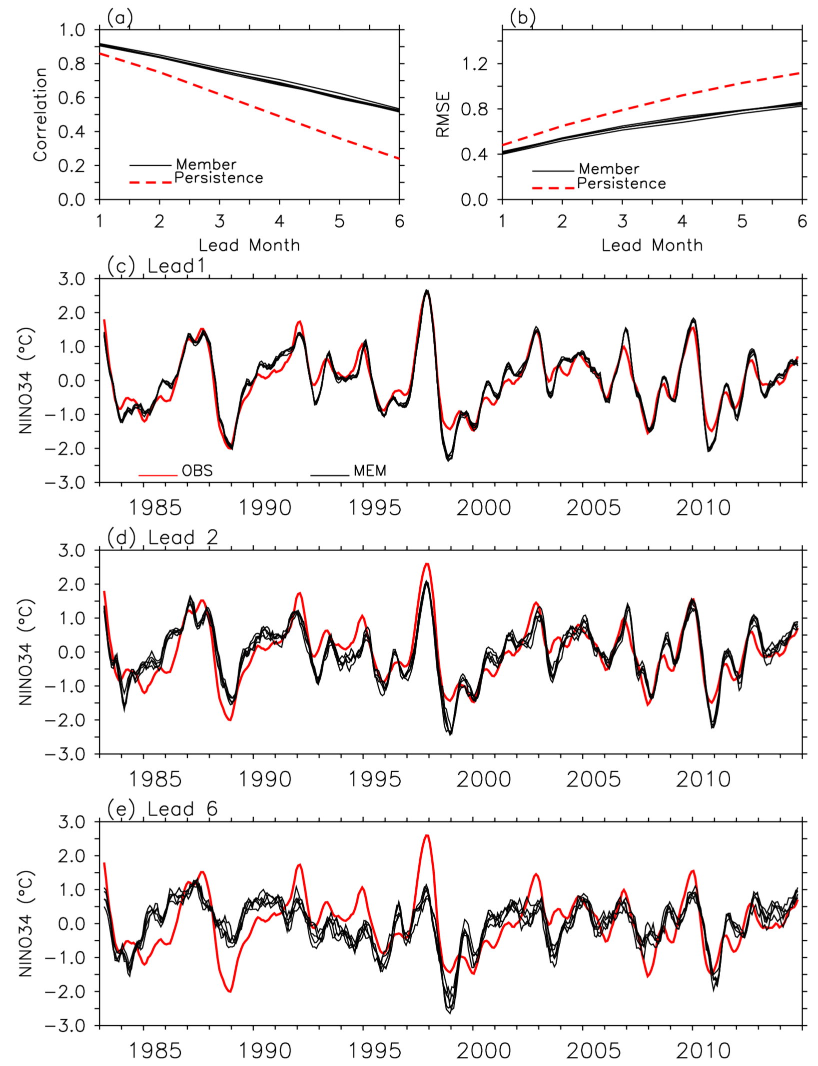

FIG. 1 (a) Anomaly temporal correlation coefficient (TCC), (b) root mean square error (RMSE) between observed and predicted Niño 3.4 indices from 1- to 6-month lead times, and time series of Niño3.4 index from observations (red line) and forecasts (black lines) at (c) 1-month, (d) 3-month, and 6-month lead times. In (a, b), TCCs and RMSEs of persistence and individual member predictions are indicated by red dashed-lines and black solid-lines, respectively. In (c-e), for a clear comparison, the 3-month running mean is applied to the Niño3.4 index before plotting.

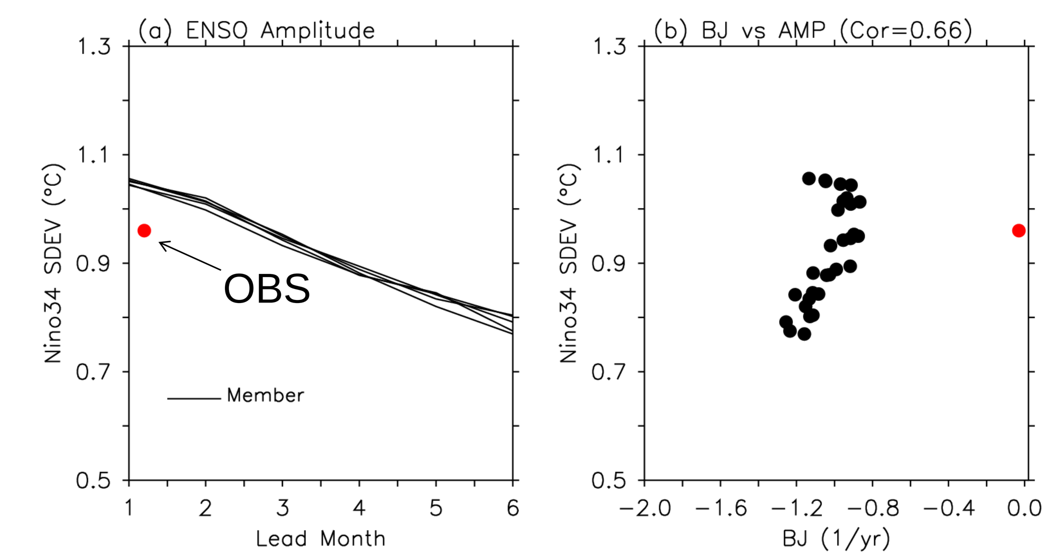

FIG. 2 (a) ENSO amplitude (° C) and (b) scatter plots of ENSO amplitude versus BJ index from 1-to 6-month lead times. Black lines and black dots relate to individual forecasts. Red dot indicates observations. In (b) correlation coefficient between BJ index and ENSO amplitude from individual forecasts is shown.

- APCC CCSM3 model can make skillful predictions for interannual ENSO events at a 6-month lead time, even with the simple wind-ocean temperature nudging initialization method
- Forecast errors in ENSO amplitude increase with forecast lead times
- ENSO amplitude change with an increase in forecast lead times is well represented by a change in the growth rate, as estimated using the BJ index.

ENSO forecast errors and mean state bias

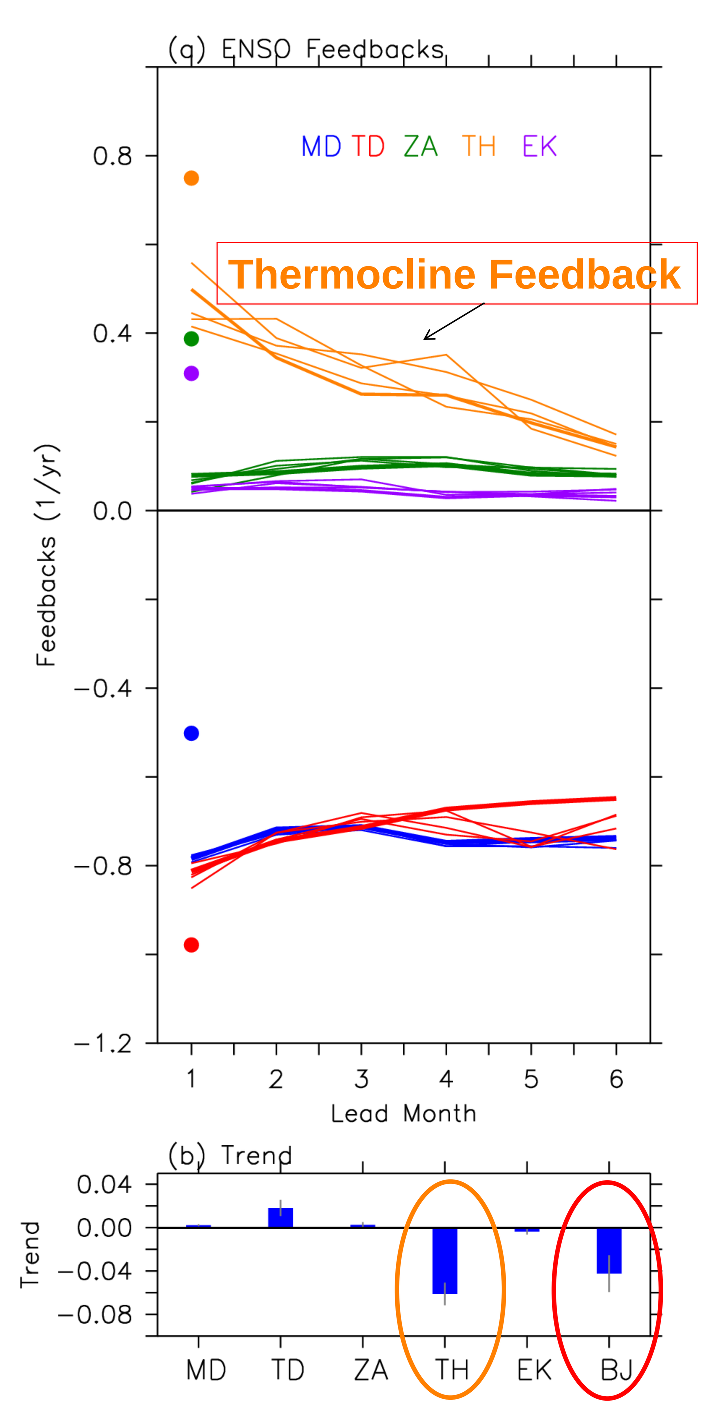

FIG. 3 (a) Feedback terms in BJ index from predictions calculated at each lead month time. Blue (lines and dot) is mean advection damping (MD), red is thermodynamic damping (TD), green is zonal advective feedback (ZA), orange is thermocline feedback (TH), and purple is Ekman feedback (EK). Colored dots indicate results from observations. Solid lines indicate results from individual forecasts. (b) Trend (yr^{-1} lead mon^{-1}) of each BJ index feedback term over forecast lead times. Blue bars show an average of all member forecasts and gray vertical lines show inter-ensemble member spread as estimated with standard deviation of trends from individual member forecasts.

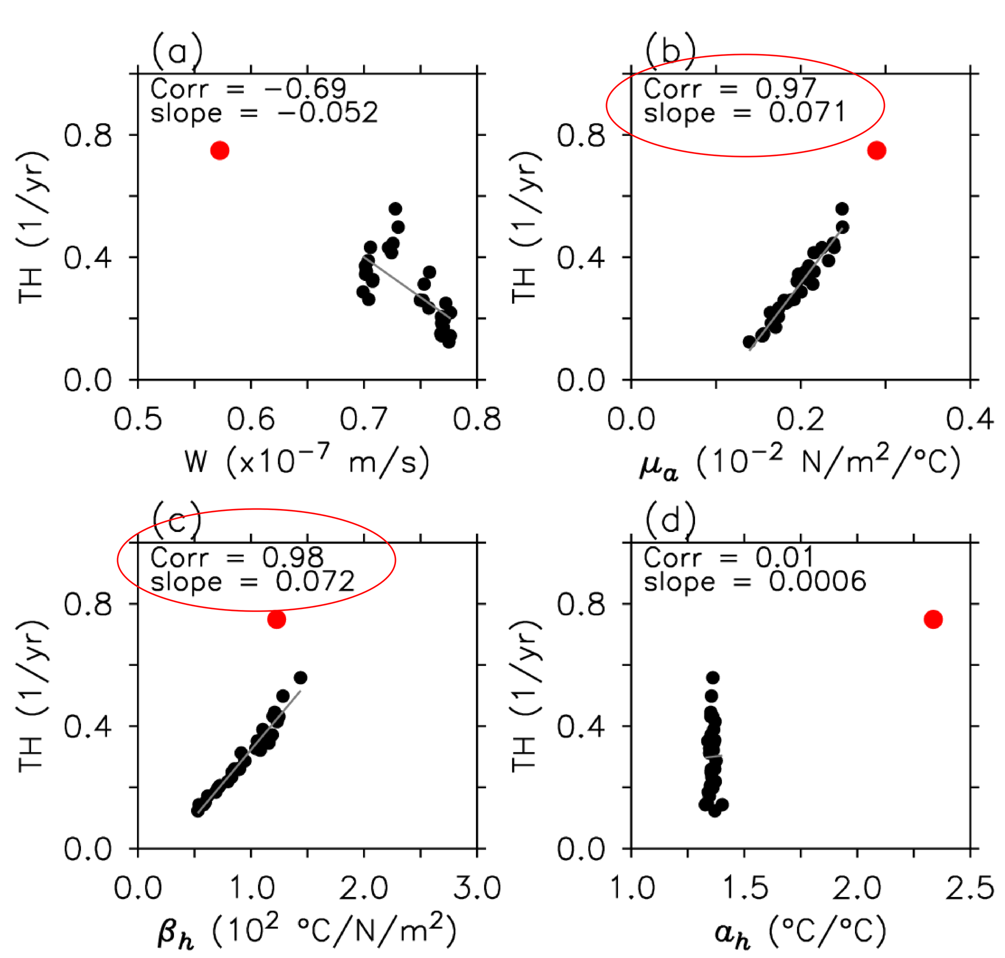

FIG. 4 Scatter plots of thermocline feedback versus its contributing factors, (a) W, (b) μ_a, (c) β_h, and (d) a_h from 1-to 6 month lead times. Black dots indicate individual member forecasts. The observed counterparts (red dots) of the thermocline feedback and contributing factors are also shown. Correlation coefficients and regression slopes, computed using samples from individual forecasts, are also shown.

$$+\mu_a \beta_h \langle -\frac{\bar{w}}{H_1} \rangle_E a_h$$

- ✓ μ_a : **wind response to a SST forcing**
- ✓ β_h : **response of the equatorial thermocline slope to a wind forcing**
- ✓ a_h :**an effect of thermocline depth changes on ocean subsurface temperature**

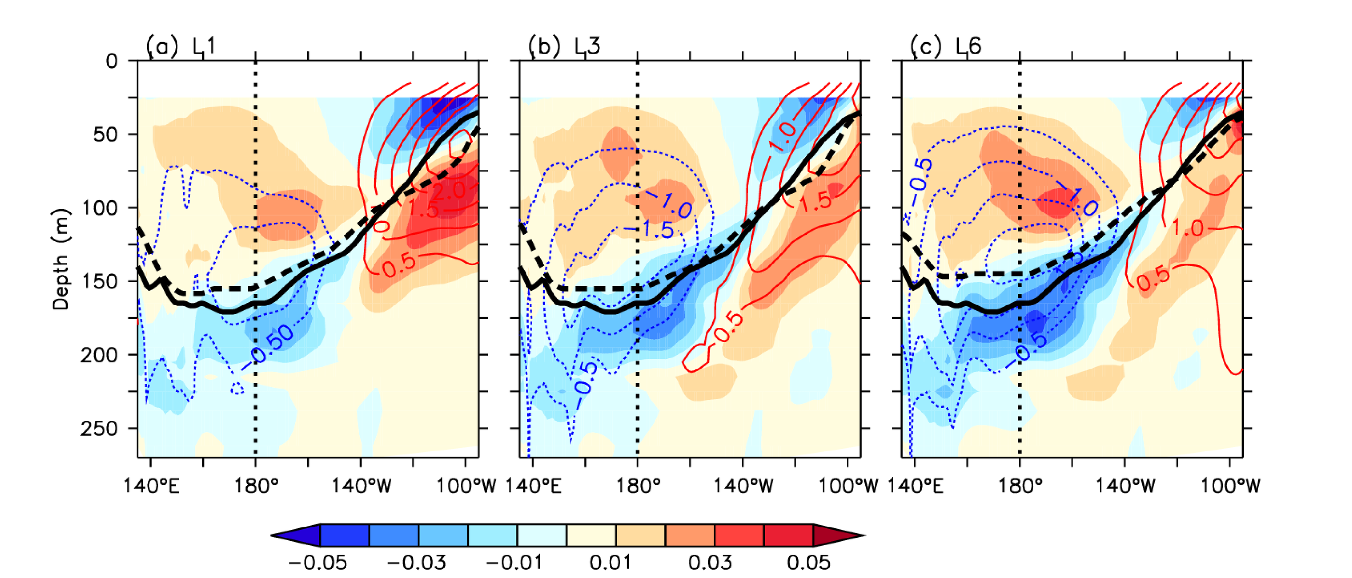

FIG. 5 Vertical cross section of difference between climatological mean ocean temperature (colored contour lines, contour interval = 0.5° C, zero lines are removed) along the equator (2° S-2° N) and its vertical gradients (shades, ° C m^{-1}) over the hindcast periods (1983–2014) from the average of all member forecasts at (a) 1-, (b) 3-, and (c) 6-month lead times, and those from the GODAS reanalysis. The thermocline depth (depth of maximum temperature gradient within 0–400 m) from forecasts (thick black dashed-lines) and the observations (thick black solid-lines) are also superimposed.

- Forecast errors in the thermocline feedback are most strongly associated with those in ENSO amplitude.
- These errors are mainly attributable to a weakened intensity of both the equatorial Pacific thermocline slope response to wind forcing, and the surface wind response to SST forcing.
- Weakened atmosphere-ocean coupling is found to be closely related with upper ocean temperature bias in the tropical Pacific, which is increased with forecast lead times, because of the enhanced upper ocean thermal stratification.
- A number of state-of-the-art coupled seasonal forecast models continue to suffer from cold bias in the tropical Pacific Ocean, and they also have certain difficulties in predicting realistic ENSO amplitude at longer lead times.
- Therefore, the results of this study strongly suggest that it is necessary to reduce tropical Pacific climate biases in coupled climate models to provide better forecasts for the intensity of ENSO events.

Statistical Downscaling of Seasonal Prediction using Weather Generator with Application to a Korea Basin in Boreal Winter

Moosup Kim (moosupkim@apcc21.org)
APEC Climate Center, Busan, Korea

Abstract

GCM is a fundamental source for predicting future climate conditions. Unfortunately, its output is too coarse in space and time to be directly applied to application studies. Currently, there is a large amount of research focused on closing the gap between resolutions of GCM output and application data. This process is called downscaling. In this study, we consider a statistical downscaling of GCM seasonal prediction into a local basin in daily time scale. Weather generator is a promising tool for this purpose. However, almost all weather generators are originally designed to simulate local weather based on climatology during observation period. Especially, inter-annual variability of climate is ignored. In this study, we develop a new weather generator linked with large-scale climate in order to reflect seasonal prediction into weather simulation. The basic strategy for this link is to parametrize local climate characteristics into the underlying weather generator model, then, to link it with large-scale climatic variables. It indicates that the values of parameters, representing the condition of local climate system, are varying according to that of large-scale climate. We illustrate it by an application to a Korea basin. Local climate characteristics under consideration are monthly mean of daily maximum/minimum temperatures adjusted by precipitation effect, mean of dry-spell length, and precipitation intensity. The link between local and large-scale climate is quantified by regression model.

Observation/Climate Data

- Weather observation data: Automatic Synoptic Observation System Data, Republic of Korea, 1988-2013,
- APCC MME Seasonal Prediction Hindcast Data for DJF issued in NOV, a month before the beginning of Boreal Winter ,
- NCEP Reanalysis Data.

Downscaling Scheme

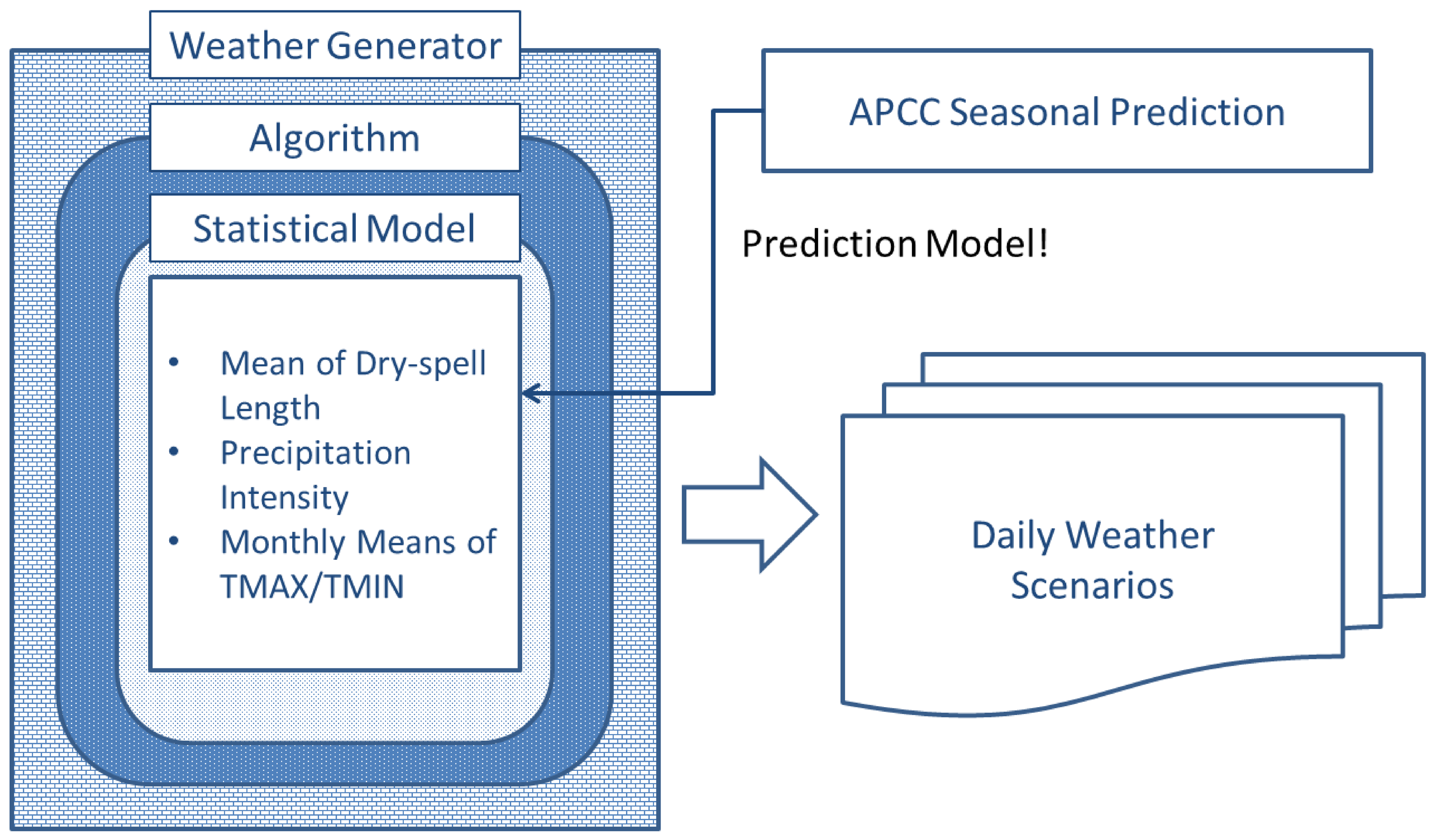

- **Parametrization**: first, we *parameterize* the underlying weather generator model to express Inter-annual variation of local basin climate.
- **Inter-annual Varying Parameters**: *Precipitation Intensity, Mean of Dry-spell Length, Monthly Means of TMAX/TMIN Adjusted by Precipitation Effect.*
- **Prediction Model**: second, we link the parameters with Seasonal Prediction of large-scale climate by *Prediction Model*. In this study, the prediction model is a system of regression equations.

Local Precipitation Model

- Basically, we model local precipitation by wet/dry-spell alternation scheme.
- Dry-spell L is modeled by negative binomial distribution with mean $\mu^L > 0$ and shape $\theta > 0$.
- *The mean $\mu^L = \mu_i^L$ (i: year) is taken as an inter-annual varying parameter.*

$$\Pr(L=m+1)=\frac{\Gamma(m+\theta)}{m!\Gamma(\theta)}\left(\frac{\mu_i^L-1}{\theta+\mu_i^L-1}\right)^m\left(\frac{\theta}{\theta+\mu_i^L-1}\right)^\theta,\quad m=0,1,2,\ldots$$

- The precipitation amount R is modeled by gamma distribution with mean $\mu^R > 0$ and shape $\alpha > 0$.
- μ^R is called precipitation intensity.
- $\mu^R = \mu_i^R$ (i: year) *is taken as an inter-annual varying parameter.*
- μ_i^R depends on site, i.e., $\mu_i^R = \mu_i^R(s)$, where s denotes site.

$$\Pr(R\le x)=\int_0^x\frac{(\alpha/\mu_i^R)^\alpha}{\Gamma(\alpha)}z^{\alpha-1}\exp\left(\frac{\alpha z}{\mu_i^R}\right)dz,\quad x>0.$$

Local Temperature Model

- Local temperature $T(s,t)$ has annually cyclic mean $\mathrm{E}\{T(s,t)\}$. $T=\mathrm{TMAX}$ or $T=\mathrm{TMIN}$. s: site, t: day.
- The deviation from cyclic mean, $T(s,t)-\mathrm{E}\{T(s,t)\}$ is modeled by regression model for precipitation effect on temperature.
- *The intercept term $\beta_{0,i}(s)$ (i: year) in the regression model is taken as an annually varying parameter representing monthly mean adjusted by precipitation effect.*

$$T(s,t)-\mathrm{E}\{T(s,t)\}=\beta_{0,i}(s)+\beta_1(s)\left\langle \mathbf{R}^\gamma(t),\Psi\right\rangle+\sigma(s,t)\cdot\varepsilon(s,t)$$

Local Temperature Model
The deviation in the left-hand is modeled by regression equation, where $\mathbf{R}(t)$: multisite precipitation, $\gamma > 0$: linearity parameter, Ψ: an EOF mode.

- Standard deviation $\sigma(s,t)$ is modeled by GLM for precipitation effect on temperature, too.
- Anomaly $\varepsilon(s,t)$ is assumed to be a vector-AR process for its spatial and temporal correlation structure. However, these are assumed to be not annually varying.

Study Area: Nakdong

- Nakdong River Basin: one of the biggest basins in Republic of Korea.
- It is covered with 14 stations, (the red-colored points in the map presented below).

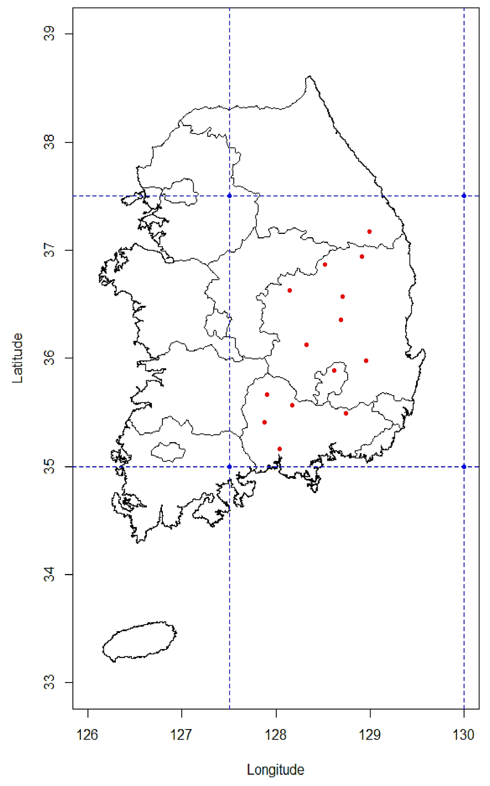

Nakdong River Basin
One of the biggest basin in Republic of Korea. 14 observation stations cover it. Weather observation data are available from 1988. Target season is DJF.

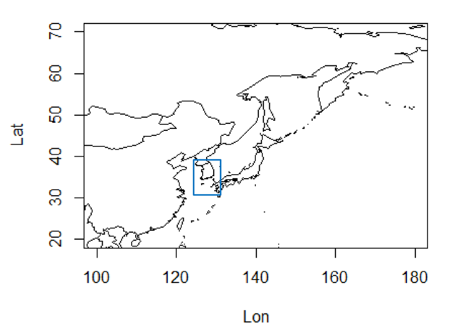

Co-variation of Inter-annually Varying Parameters

- Though $\mu_i^R(s)$ and $\beta_{0,i}(s)$ (i: year) are estimated at each site s, separately, they reveal co-variation since the sites lie in the same basin.
- For prediction model, it is effective and efficient to take their first-order EOF coefficients as predictand.

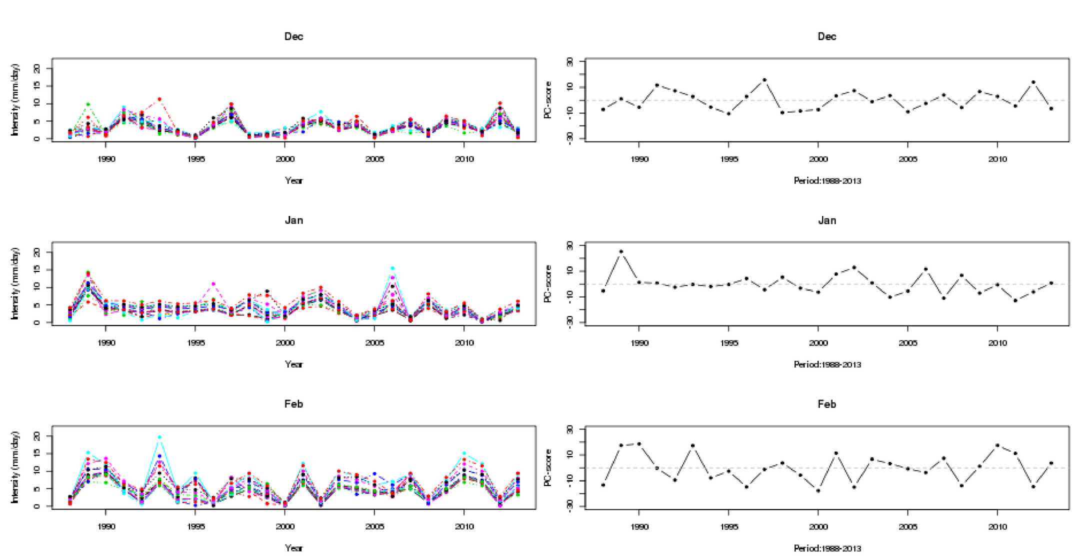

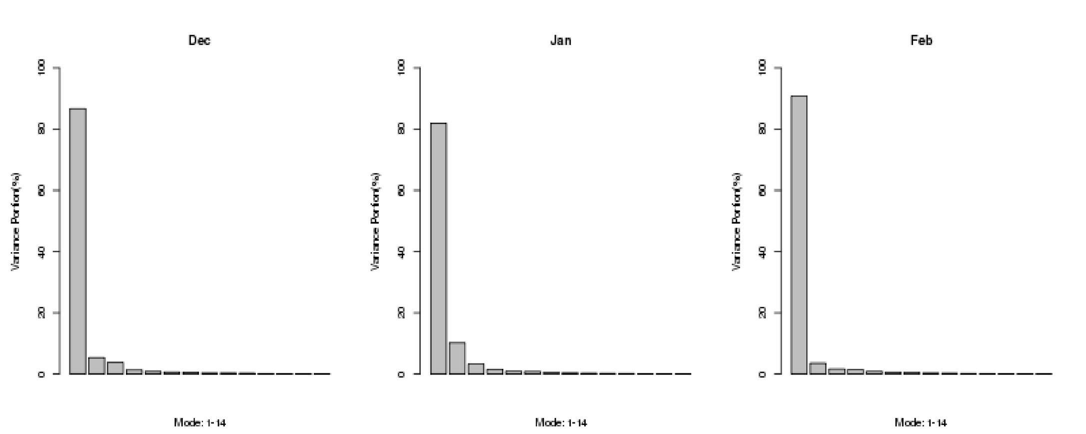

Left-hand in the Top: annual time series of precipitation intensities (mm) of all sites in a basin for each month DJF. They appear to move together.

Right-hand in the Top: annual time series of the first-order EOF coefficients. They represent annual co-variation well, thus, are taken as predictands in prediction model.

Bottom: The result of EOF analysis for each month. Indeed, the variance of the first-order mode occupies around 90% of total variance.

Prediction Model

- Through an exploratory analysis, we choose Z500 and SLP as predictors
- We consider regression equations for prediction model.
- For mitigating overfitting, some regularization techniques are employed: Regularized Canonical Correlation Analysis (RCCA) and LASSO variable selection.

Inter-annual Variation of Predictands

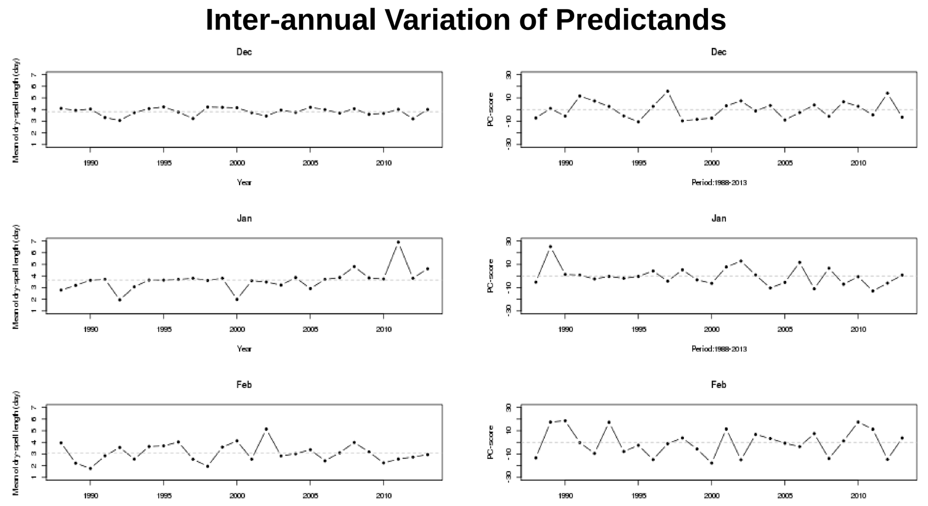

Mean of Dry-spell length

The first-order EOF coefficients of Precipitation Intensity

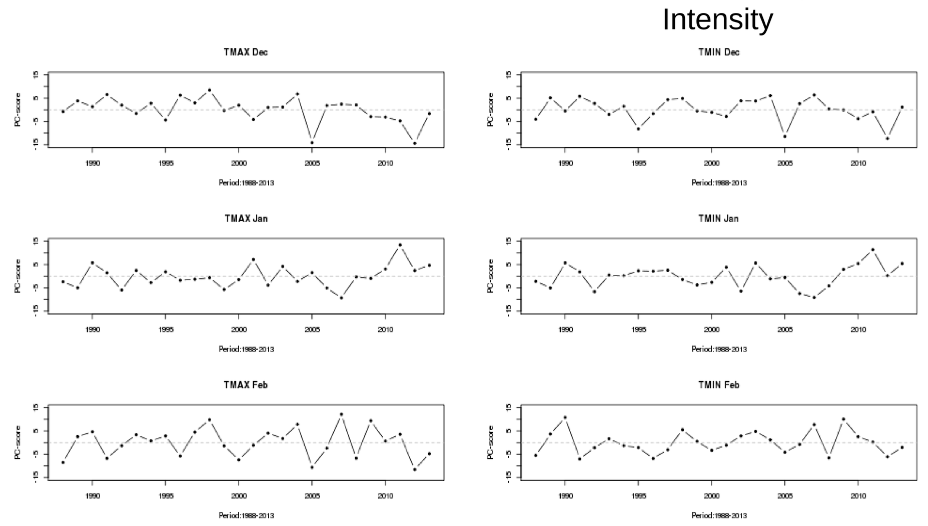

The first-order EOF coefficient of TMAX Intercept

The first-order EOF coefficient of TMIN Intercept

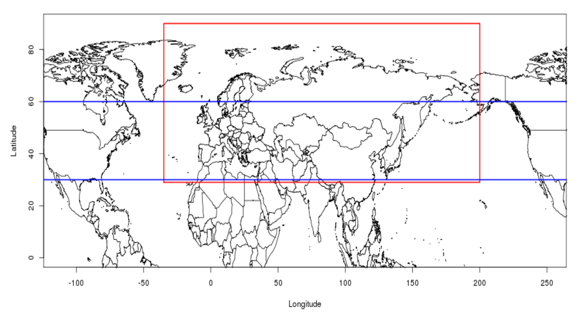

The Domains of the Predictors:
Red box: Z500,
Blue box: SLP.

Regression Equation for Prediction

- Y_i: predictand, $Z_i^{(l)}$: the l-th GCM prediction field, i: year, $l=1,\ldots,6$, (6 GCMs provide the seasonal prediction).
- $\varphi_j^{(l)}$: the j-th coefficient vector of the l-th GCM prediction field which is from RCCA with Reanalysis data.
- LASSO method is applied to the regression fitting for deleting insignificant predictors.

$$Y_i=\beta_0+\sum_{l=1}^{6}\sum_{j=1}^{10}\beta_{l,j}\left\langle Z_i^{(l)},\varphi_j^{(l)}\right\rangle+\varepsilon_i\,.$$

Regression Equation for Prediction
For mitigating overfitting, regularization techniques are applied.

Month	Predictand	Predictor	MSE ratio	Correlation
Dec	The First EOF coefficient of TMAX intercepts	Z500	0.80	0.36
	Mean of Dry-spell Length	SLP	0.67	0.60
	The First EOF coefficient of Intensities	SLP	0.66	0.53
Feb	The First EOF coefficient of TMAX intercepts	Z500	0.89	0.18

Plot of Predictands (y-axis) vs. Leave-one-out Predicted Values (x-axis)

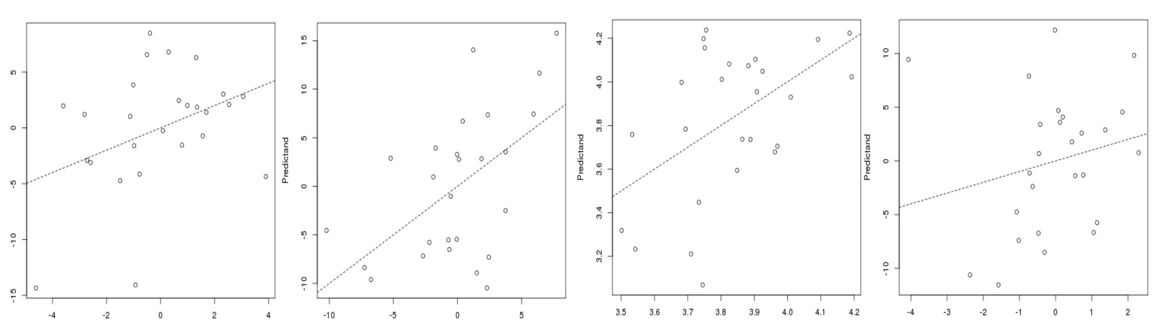

TMAX intercept in DEC. corr: 0.36

Precipitation Intensity in DEC. corr: 0.53

Mean of Dry-spell Length in DEC. corr: 0.60

TMAX intercept in FEB. corr: 0.18

Acknowledgements

This research was supported by the APEC Climate Center.

Detection of Changes in Indicators of Hydrologic Alterations Under CMIP5 Projections from a Model Chain with a Multi-Model Approach

Hyung-Il Eum (hieum01@apcc21.org), Hyo-Jin Lee (ssaddari@apcc21.org)

Climate Application Department, APEC Climate Center, 12 Centum 7-ro, Haeundae-gu Busan, Republic of Korea

GC13F-1253

Introduction

Multi-decadal climate projections provide fundamental information to foresee how the earth system may be altered by climate change. Recently climate change studies have paid attention to assessment of climate change impacts at regional or local scales. Due to the mismatch of spatial resolution between (global and regional) climate models and regional applications, however, downscaling methods have been employed to produce a finer scaled and bias-corrected climate projections. This study applied long-term preserving statistical downscaling methods. Using the downscaled climate conditions, hydrological projections are produced to detect alterations in hydrologic regimes using a set of hydrologic indicators. Based on multiple Representative Concentration Pathways (RCPs), GCMs, downscaling methods, and hydrologic models, this study set up a model chain to investigate the changes in indicators of hydrologic alterations (IHAs) during three future time windows at multi-purpose reservoirs in major river basins over South Korea.

Climate and hydrologic data

- 26 CMIP5 daily precipitation, minimum & maximum temperature
- Downscaled at 60 stations for Ref.(1976-2005), 2020s(2006-2035), 2050s(2036-2065), 2080s(2066-2095)
- 7 hydro-stations in 5 river basins

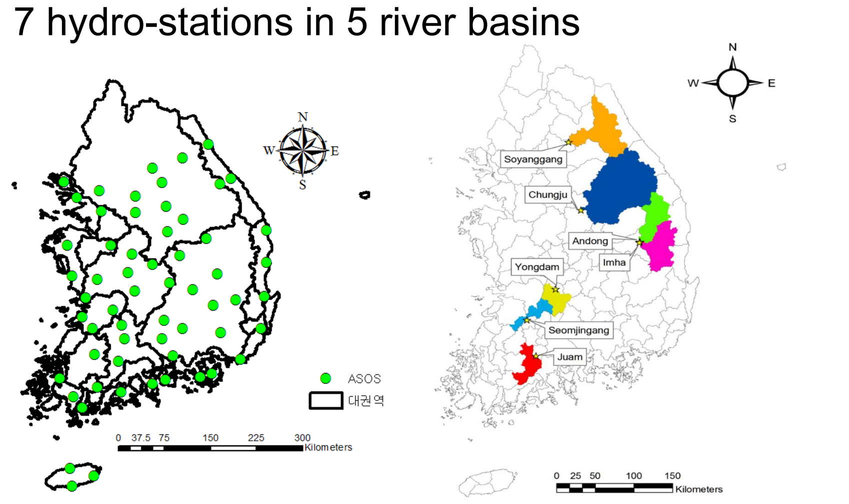

No.	GCMs	Resolution	Institution
1	CMCC-CM	0.750 x0.748	Centro Euro-Mediterraneo per I Cambiamenti Climatici
2	CMCC-CMS	1.875x1.865	
3	CCSM4	1.250x0.942	National Center for Atmospheric Research
4	CESM1-BGC	1.250x 0.942	
5	CESM1-CAM5	1.250x0.942	
6	MRI-CGCM3	1.125x 1.122	Meteorological Research Institute
7	CNRM-CM5	1.406x 1.401	Centre National de Recherches Meteorologiques
8	HadGEM2-AO	1.875x1.250	Met Office Hadley Centre
9	HadGEM2-CC	1.875x1.250	
10	HadGEM2-ES	1.875x1.250	
11	INM-CM4	2.000x1.500	Institute for Numerical Mathematics
12	IPSL-CM5A-MR	2.500x 1.268	Institut Pierre-Simon Laplace
13	MPI-ESM-LR	1.875x 1.865	Max Planck Institute for Meteorology (MPI-M)
14	MPI-ESM-MR	1.875x1.865	
15	FGOALS-s2	2.813x1.659	LASG, Institute of Atmospheric Physics, Chinese Academy of Sciences
16	NorESM1-M	2.500x1.895	Norwegian Climate Centre
17	GFDL-ESM2G	2.500x 2.023	Geophysical Fluid Dynamics Laboratory
18	GFDL-ESM2M	2.500x2.023	
19	BCC-CSM1-1	2.813x2.791	Beijing Climate Center, China Meteorological Administration
20	BCC-CSM1-1-M	1.125x1.122	
21	IPSL-CM5A-LR	3.750x1.895	Institut Pierre-Simon Laplace
22	IPSL-CM5B-LR	3.750x1.895	
23	MIROC5	1.406x1.401	Atmosphere and Ocean Research Institute, National Institute for Environmental Studies, and Japan Agency for Marine-Earth Science and Technology
24	MIROC-ESM-CHEM	2.813x2.791	
25	MIROC-ESM	2.813x2.791	
26	CanESM2	2.813x2.791	Canadian Centre for Climate Modelling and Analysis

Methodology

Statistical downscaling methods

- BCSD and BCCA
- Quantile Mapping (QM): "Variance inflation" by extrapolation
- Detrended Quantile Mapping (DQM)
- Quantile Delta Mapping (QDM)

Inflation by QM

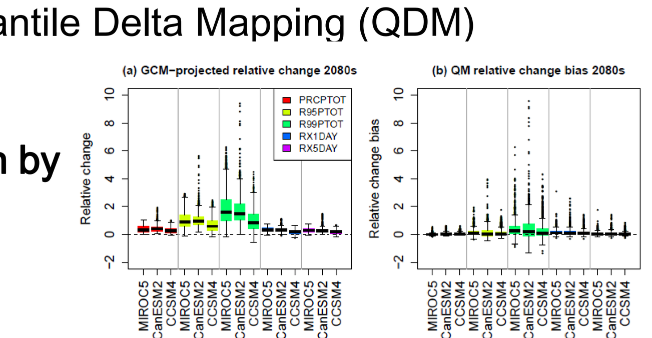

DQM

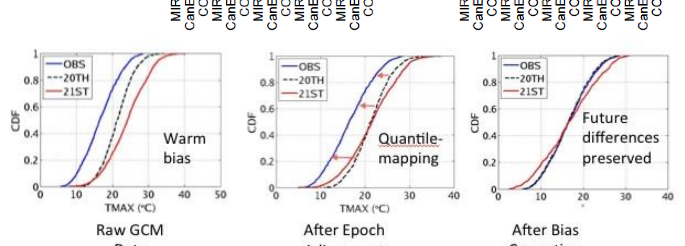

QDM

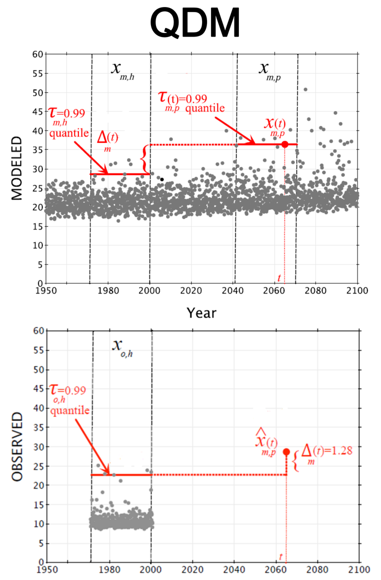

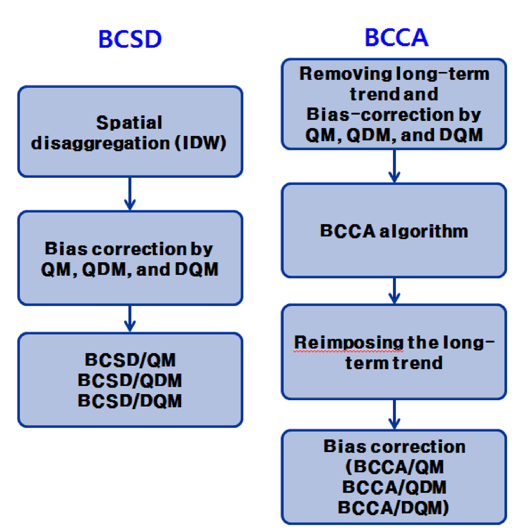

Cannon et al. (2015)

Hydrologic models

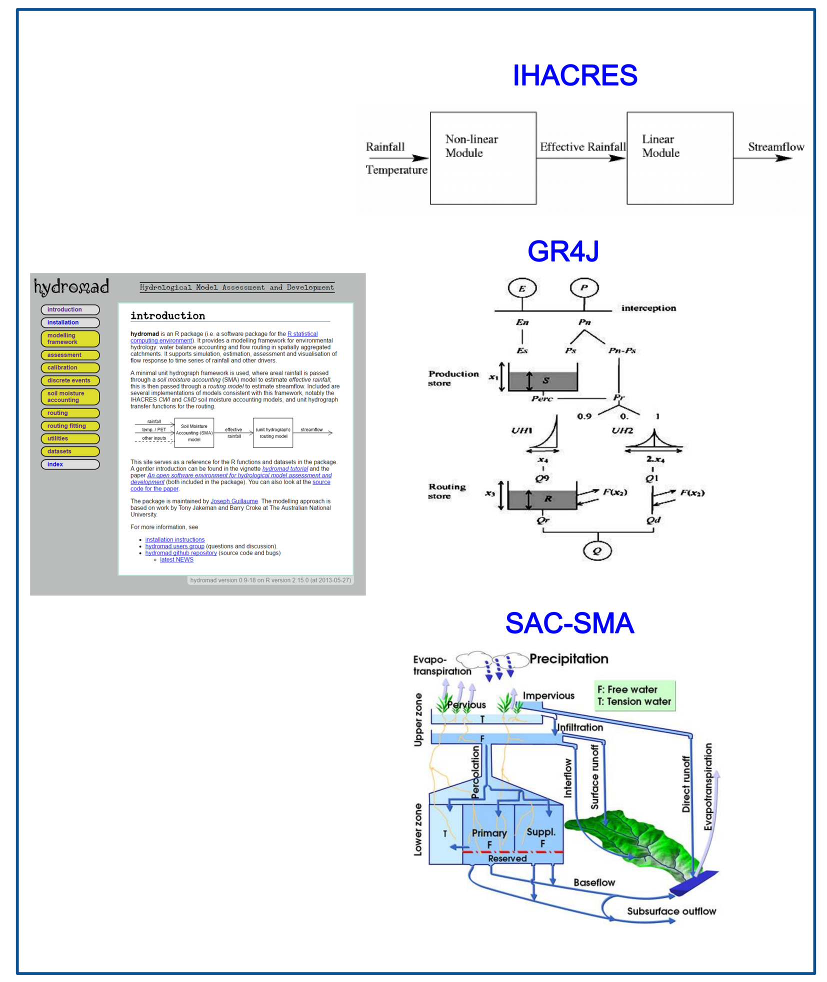

Catchment	Name of period	Period
Andong	HP1	1977/01/01 – 1987/12/31
	HP2	1987/01/01 – 1997/12/31
	HP3	1997/01/01 – 2007/12/31
	HP4	2007/01/01 – 2015/12/31
Chungju	HP1	1986/01/01 – 1996/12/31
	HP2	1996/01/01 – 2006/12/31
	HP3	2006/01/01 – 2015/12/31
Imha	HP1	1993/01/01 – 2003/12/31
	HP2	2003/01/01 – 2015/12/31
Juam	HP1	1991/01/01 – 2001/12/31
	HP2	2001/01/01 – 2015/12/31
Seomjin	HP1	1975/01/01 – 1985/12/31
	HP2	1985/01/01 – 1995/12/31
	HP3	1995/01/01 – 2005/12/31
	HP4	2005/01/01 – 2015/12/31
Soyang	HP1	1974/01/01 – 1984/12/31
	HP2	1984/01/01 – 1994/12/31
	HP3	1994/01/01 – 2004/12/31
	HP4	2004/01/01 – 2015/12/31
Yongdam	HP1	2001/01/01 – 2008/12/31
		2/31

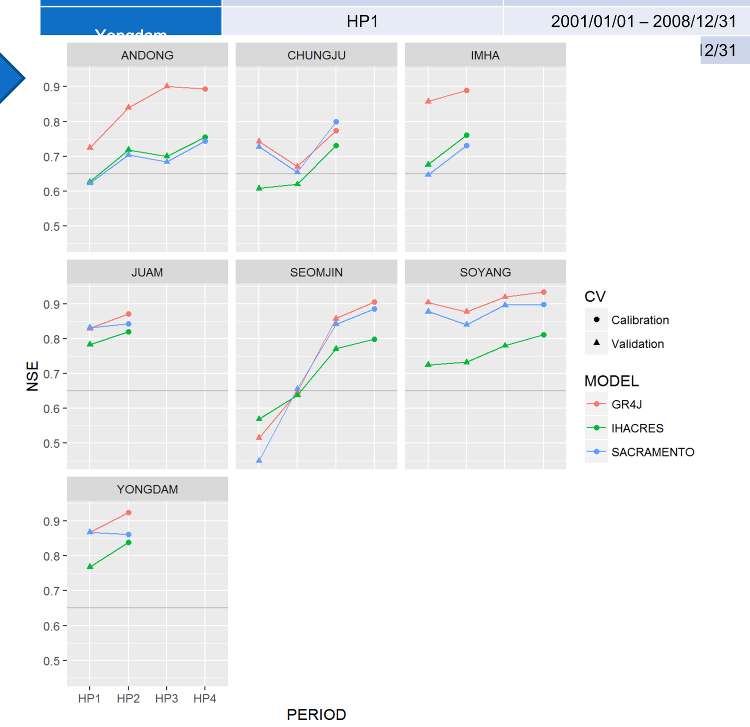

Model Chain

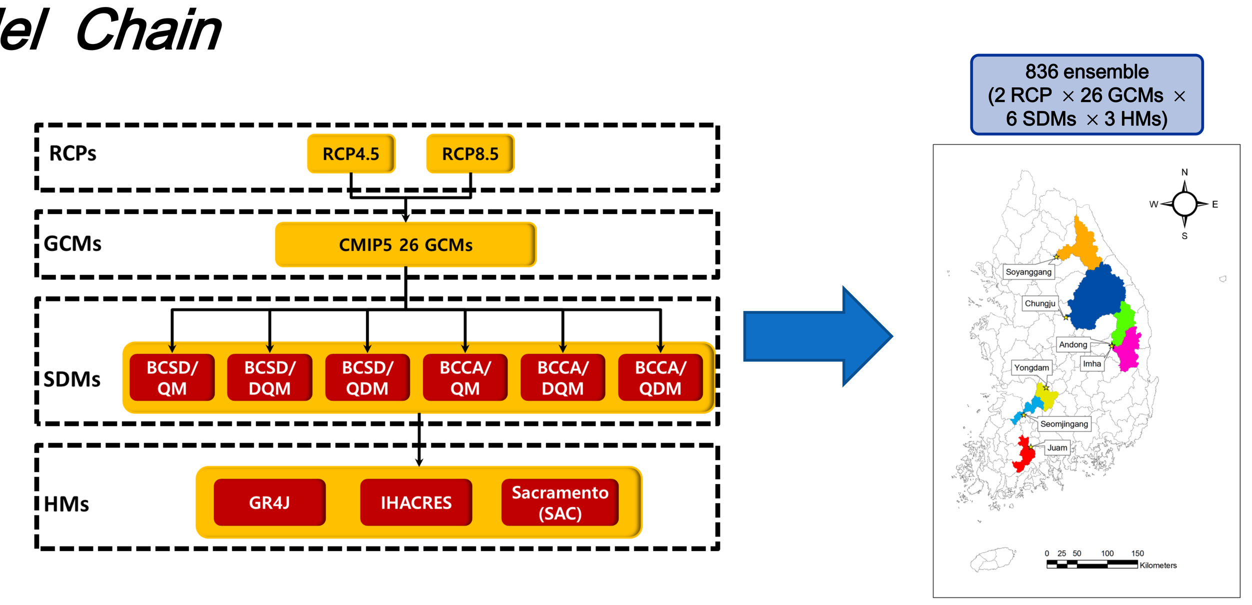

Results

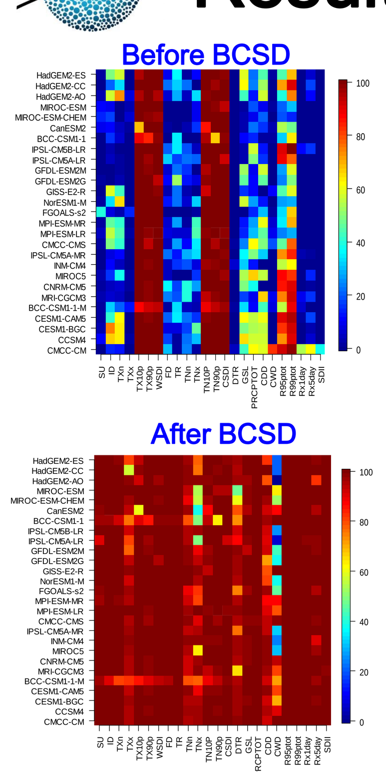

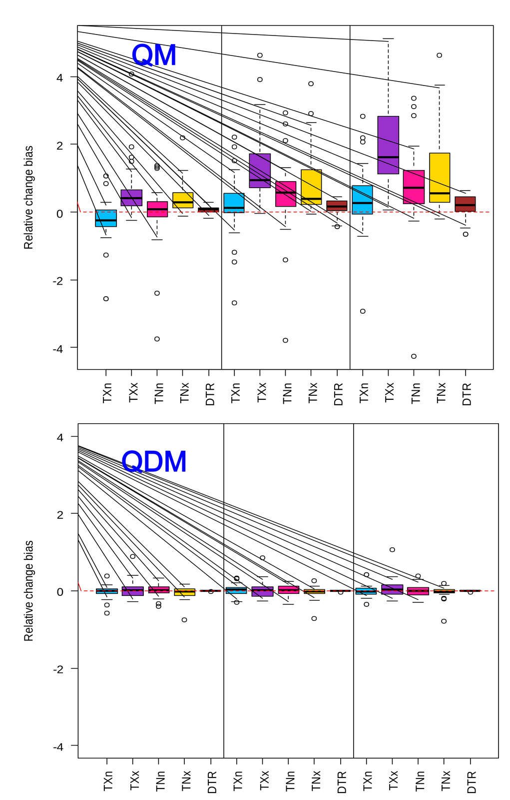

Eum and Cannon (2016)

No.	ID	Related variable	Description	Unit
1	SU	TMAX	Summer day, TMAX > 25°C	Days
2	ID		Ice days, TMAX < 0°C	Days
3	TX_n		Min TMAX	°C
4	TX_x		Max TMAX	°C
5	TX10p		Cool days, TMAX < 10th percentile	%
6	TX90p		Warm days, TMAX > 90th percentile	Days
7	WSDI		Warm spell duration, TMAX > 90th percentile	Days
8	FD	TMIN	Frost days TMIN < 0°C	Days
9	TR		Tropical nights, TMIN > 20°C	Days
10	TN_n		Min TMIN	°C
11	TN_x		Max TMIN	°C
12	TN10p		Cool nights, TMIN < 10th percentile	%
13	TN90p		Warm nights, TMIN > 90th percentile	%
14	CSDI		Cold spell duration, TMIN < 10th percentile	Days
15	DTR	TMAX & TMIN	Diurnal temperature range	°C
16	GSL		Growing season length	Days
17	CDD	PRCP	Consecutive dry days, PRCP < 1mm	Days
18	CWD		Consecutive wet days, PRCP ≥ 1mm	Days
19	PRCPTOT		Annual total PRCP in wet days (daily PRCP ≥ 1mm)	mm
20	Rx1day		Max 1-day precipitation	mm
21	Rx5day		Max 5-day precipitation	mm
22	R95pTOT		Annual total PRCP when daily PRCP > 95 percentile	mm
23	R99pTOT		Annual total PRCP when daily PRCP > 99 percentile	mm
24	SDII		Simple daily intensity index	mm/day

Time series of extreme climate indices

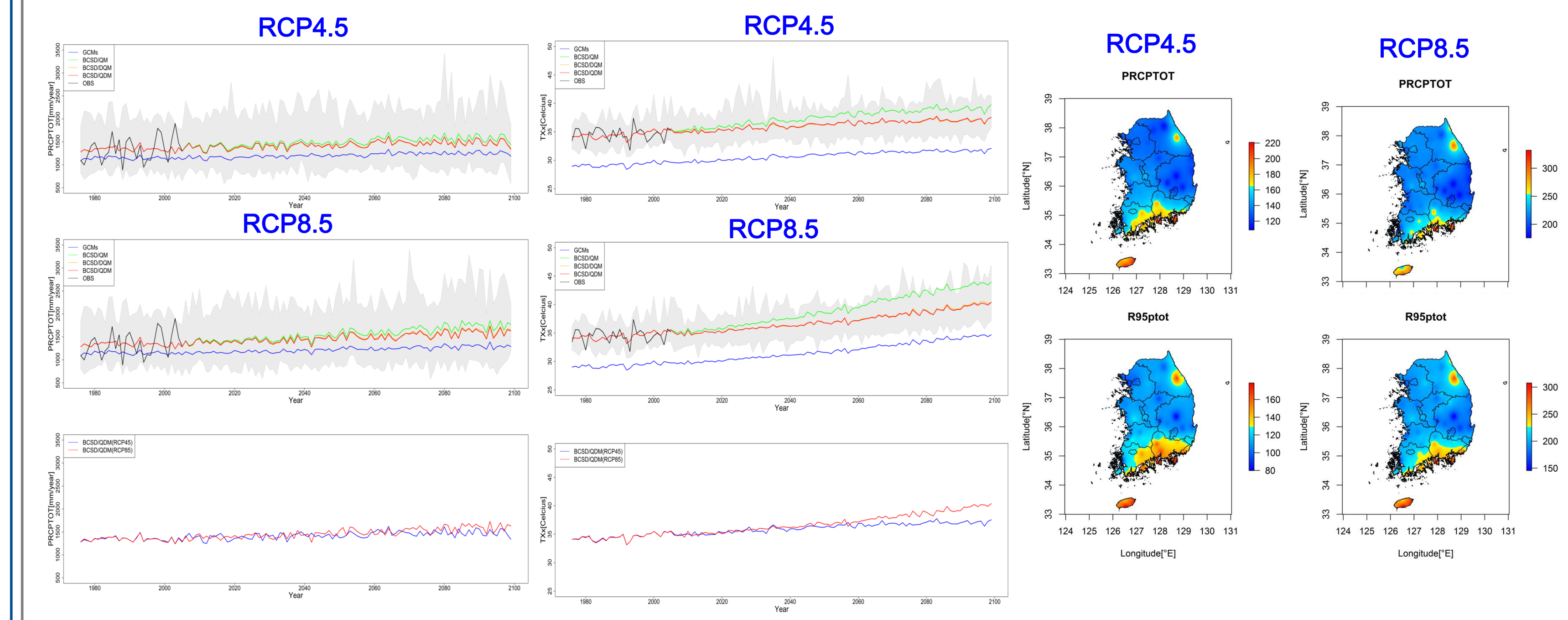

Hydrologic Alteration Factor(HAF)

$$HAF = \frac{F_p - F_r}{F_r}$$

F_p: Projected frequency

F_r: Reference frequency

Indicators	No	Examples of hydrological influence	Examples of ecological influence
Annual volume (m³), median seasonal flows	5	Annual and seasonal water volume, and center timing of the annual flow mass	Availability and suitability of habitat for aquatic organisms
Monthly flow (m³/s)	12	Magnitude of monthly water availability	Suitable habitat availability; influence on secondary variables
Annual 1-day, 7-day, 90 -day minimum and maximum (m³/s)	6	Magnitude of annual flood and drought conditions	Duration of stressful conditions

Chungju

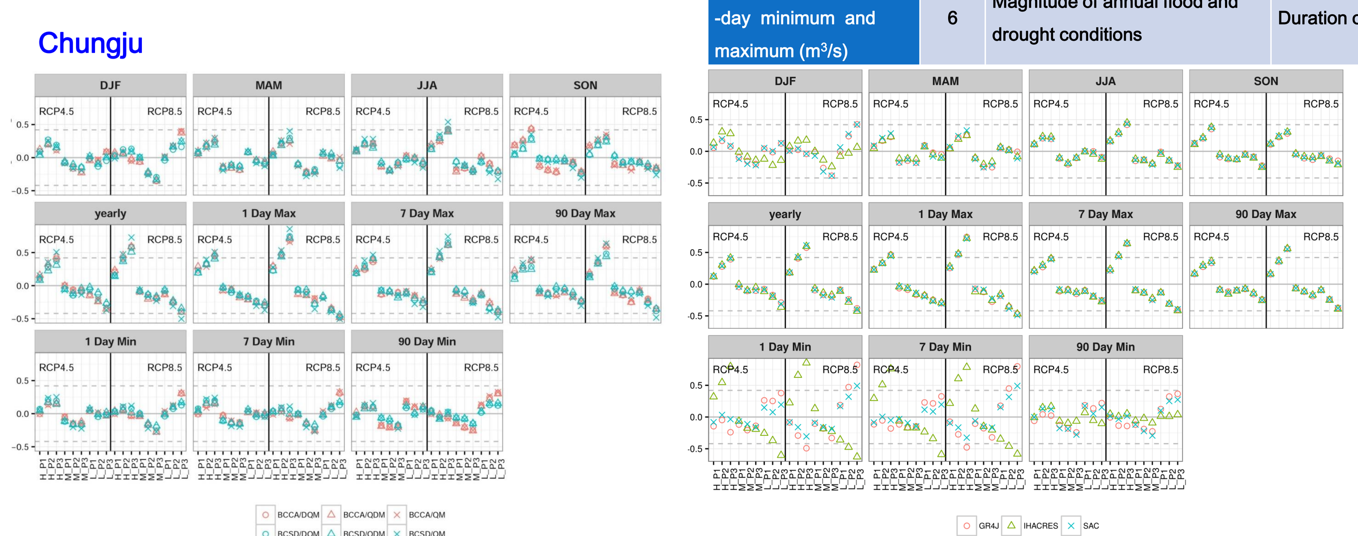

Summary

- Improvement of performance by statistical downscaling methods
- QDM preserves GCM-driven long-term trend
- Increasing in seasonal and annual flows with polarized flows in winter
- Not considerable variability between statistical downscaling methods
- Significant variability in minimum flows by the choice of hydrologic models

Reference

- Cannon, A. J., S. R. Sobie, and T. Q. Murdock, 2015: Bias Correction of GCM Precipitation by Quantile Mapping: How Well Do Methods Preserve Changes in Quantiles and Extremes? Journal of Climate, 28, 6938–6959, doi:10.1175/JCLI-D-14-00754.1
- Eum, H.-I., and A. J. Cannon, 2016: Intercomparison of projected changes in climate extremes for South Korea: application of trend preserving statistical downscaling methods to the CMIP5 ensemble. International of Journal of Climatology, DOI: 10.1002/joc.4924

Validation of Soil Water Content Estimation Method on Agricultural Regions in South Korea

Yonghee Shin(shin.yonghee@apcc21.org), Miah Kim(makim0820@apcc21.org)
Climate Application Department, APEC Climate Center, 12 Centum 7-ro, Haeundae-gu Busan, Republic of Korea

EP41C-0918

Introduction

The continuous water stress caused by decrease of soil water has a direct influence to the crop growth in a upland crop area. The agricultural drought is occurred if water requirement is not supplied timely in crop growth process. A soil moisture sensor is used to observe a change of the soil water contents. However, it's price is high and hard to apply to a wide area and sometimes an error occurs by the sensor trouble. It is more important to understand the soil characteristics for high accuracy soil moisture estimation because of the soil water contents largely depends on soil properties. The RDA(Rural Development Administration) has provided real-time soil moisture observations corrected for 71 points in the South Korea. In this study, we developed a soil water content estimation method that considered soil hydraulic parameters for the observation points of soil water content in agricultural regions operated by the RDA. SWAP(Soil-Water-Atmosphere-Plant) model was used in the estimation of soil water contents. The soil hydraulic parameters that is the input data of the SWAP model were estimated using the ROSETTA model developed by the U.S. Department of Agriculture(USDA). For the verification of soil water content estimation method, we used Haenam KoFlux observation data that are observed long-term soil water contents over 2009-2015(2014 missing) years.

Data (Soil and Weather)

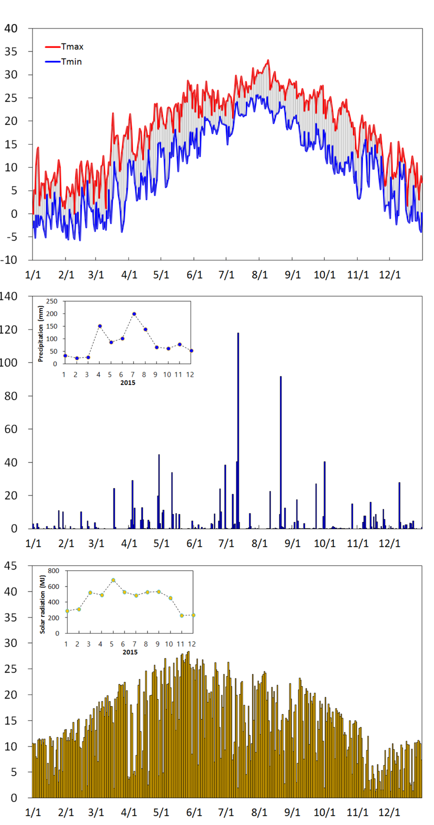

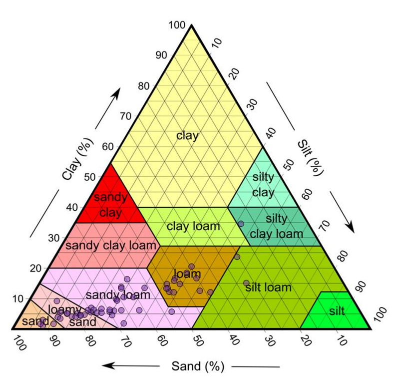

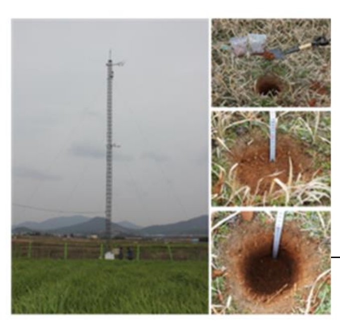

Haenam KoFlux (HFK) site

Sand:38.5% Silt: 31.5% Clay: 30.0%

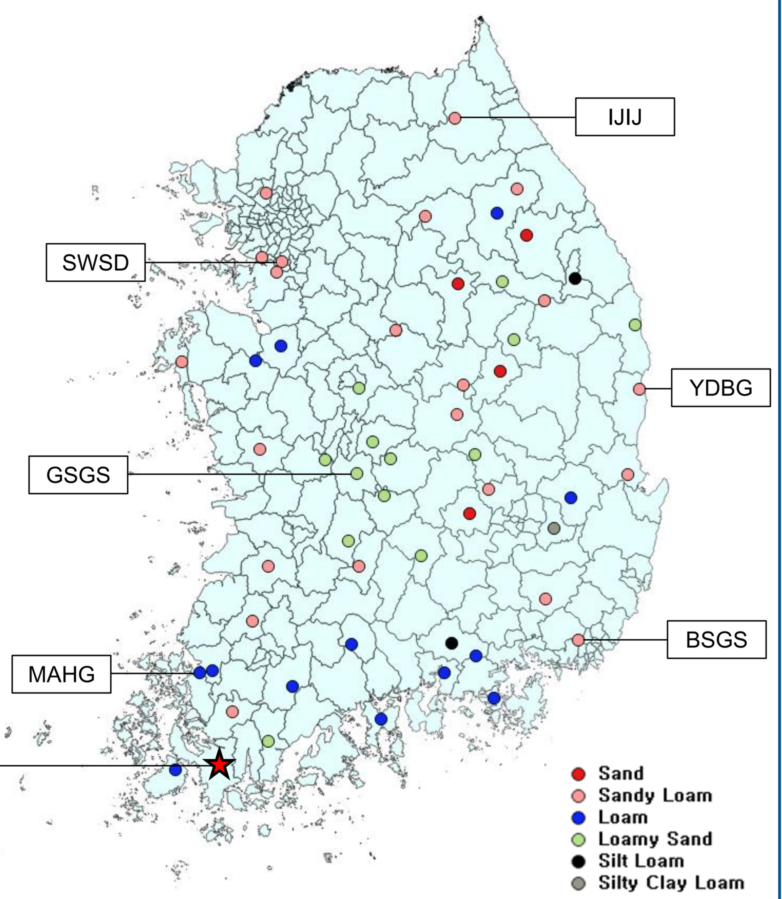

RDA soil moisture observation sites

Methodology

Estimation of soil hydraulic parameters

Rosetta Model (Schaap et al., 1999)
(Artificial Neural Networks)

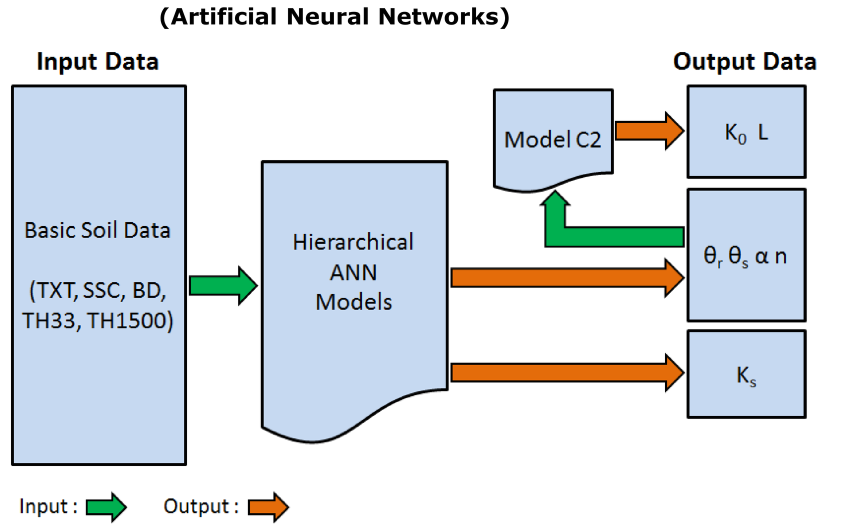

Soil hydraulic parameters

- K_s(cm/day) Saturated hydraulic conductivity
- K_0(cm/day) Unsaturated hydraulic conductivity
- θ_s(cm³/cm³) Saturated water content
- θ_r(cm³/cm³) Residual water content
- α(1/cm), n(-) Curve shape parameter

TXT : Soil Textural class (Sand, clay loam, silt) TH33 : Water contents at 33 kPa
SSC : Sand, Silt and Clay Percentages TH1500 : Water contents at 1500 kPa
BD : Bulk density

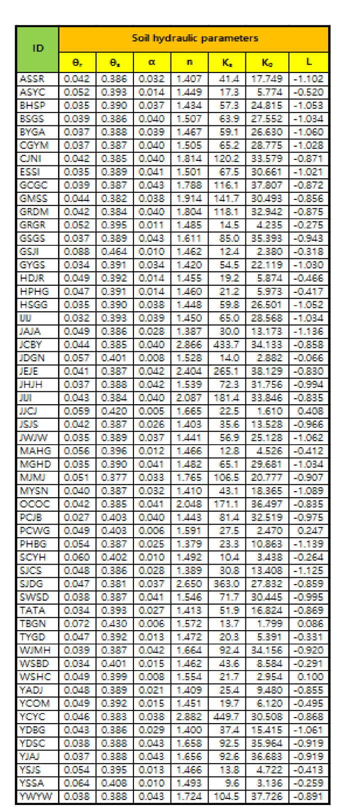

Simulation of soil water content

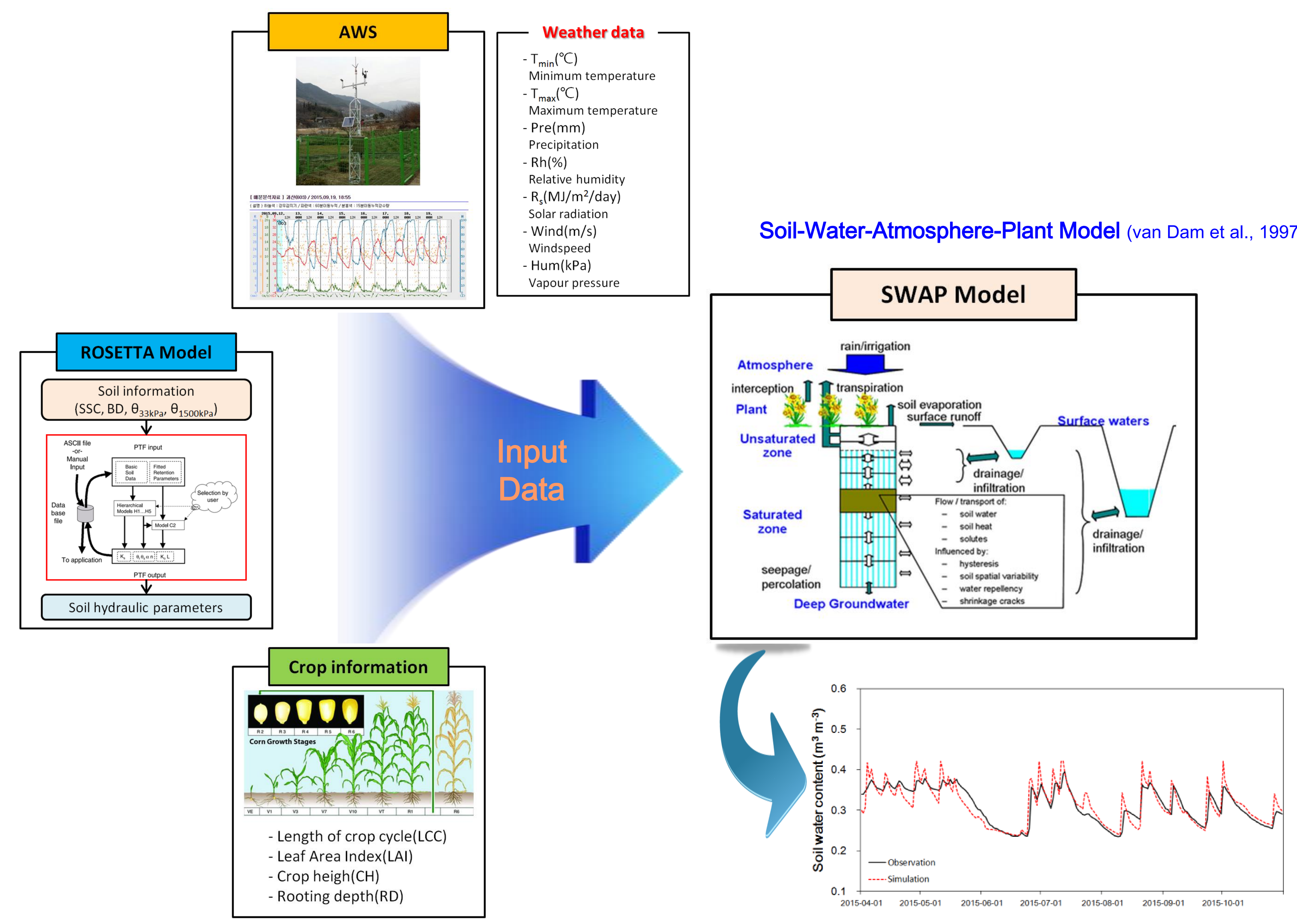

Results

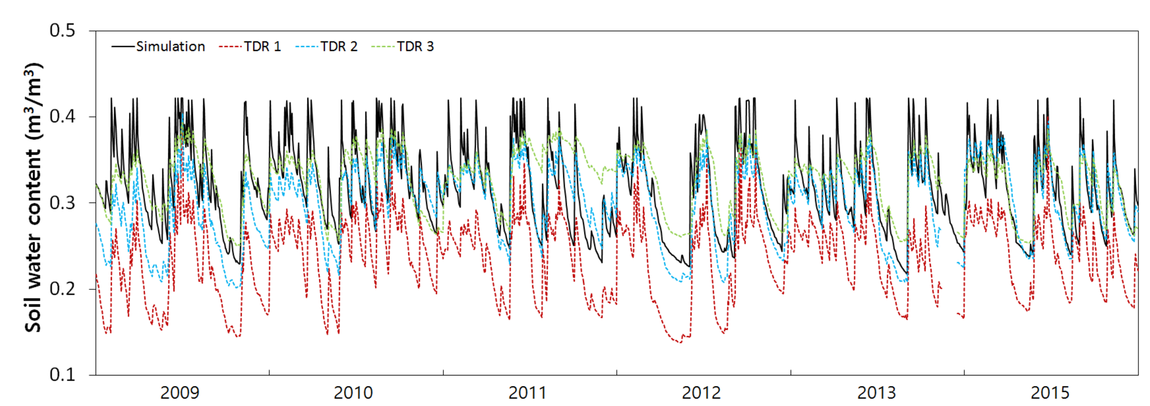

Sensor	Average
Simulation	0.318
TDR1	0.236
TDR2	0.302
TDR3	0.323

Soil water content data(TDR1, TDR2, TDR3) and SWAP simulation result at HFK site

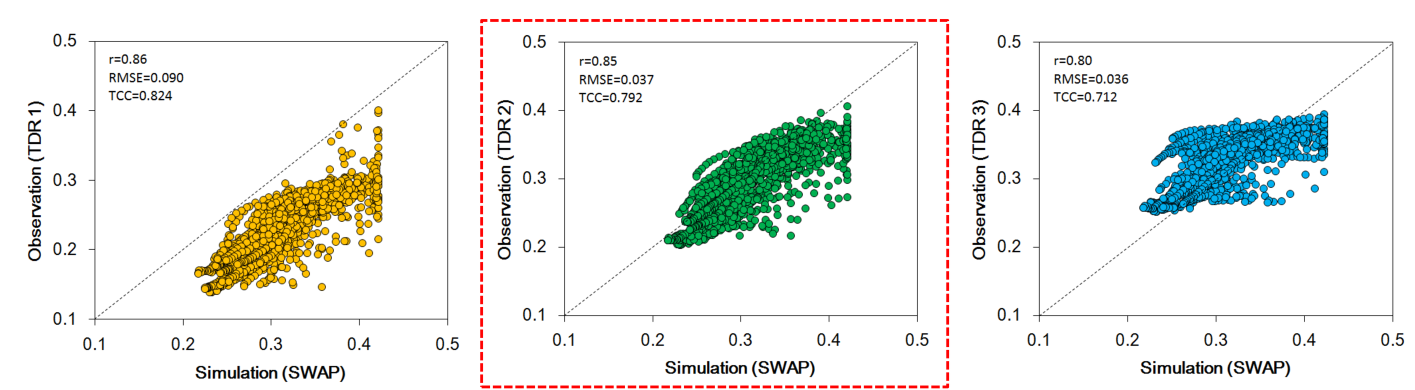

Correlation between observation and simulation results (TDR1-SWAP, TDR2-SWAP, TDR3-SWAP) at HFK site

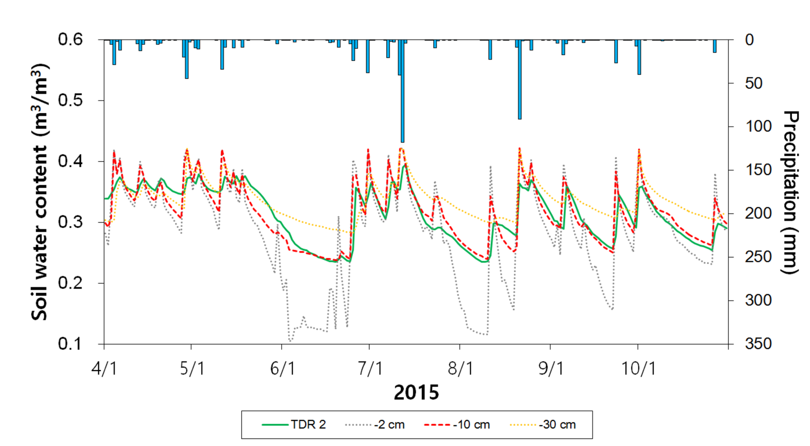

Soil water content observation data(TDR2 at -10cm depth) and soil layer simulation results at HFK site

Validation of HFK site

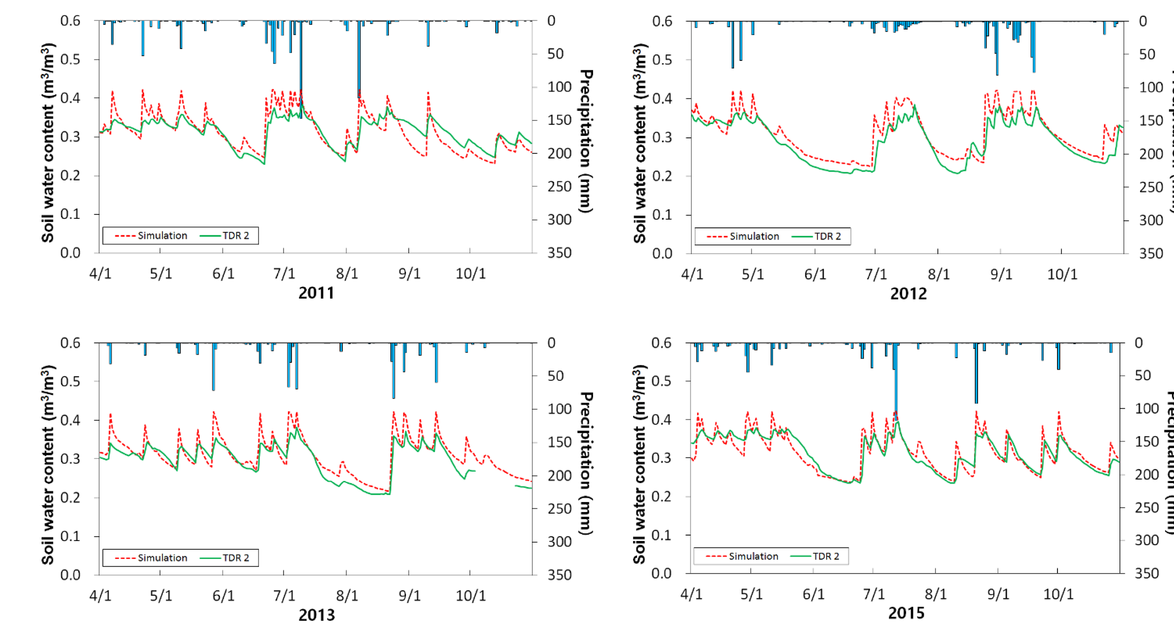

Year	R²	RMSE	TCC
2011	0.674	0.029	0.821
2012	0.789	0.034	0.888
2013	0.780	0.028	0.882
2015	0.721	0.026	0.849

In order to verify the soil water content estimation method, observation and simulation data were compared for each year.

Simulation results are in good agreement with observations as a whole, especially in 2012 and 2015 when rainfall was small over a long period.

Validation of RDA sites

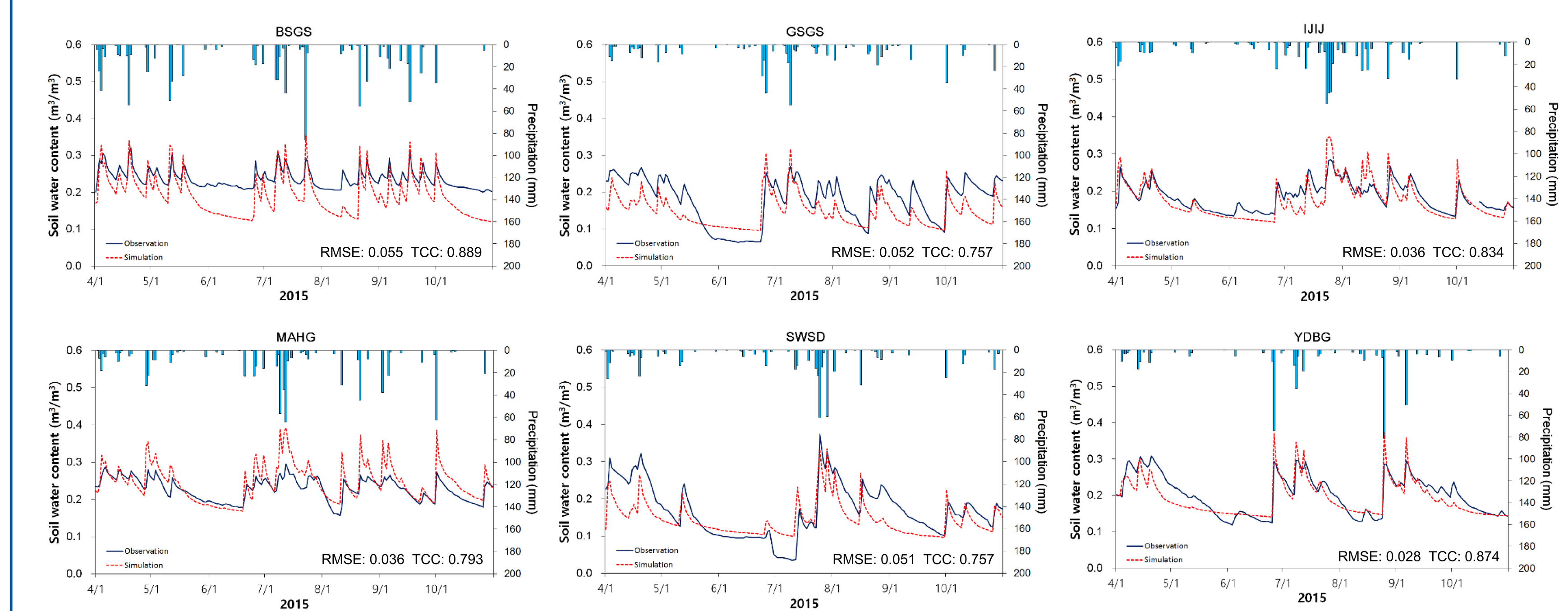

Comparison of soil water content observation data and SWAP simulation results at agricultural regions in South Korea

Summary

- Soil water content estimation method was developed for each crop growing season and the accuracy and reliability of this method were evaluated through comparison with long term observation data.
- As a result of verifying the soil water content estimation method for the observation sites, the field application was verified at a satisfactory level, but the soil with the sand content of 90% or more was in error.
- It is expected to be able to cope with water stress risk of crops if estimating soil water content by applying the weather and soil characteristics information to the proved soil water content estimation technique.

Reference

Schaap, M. G., Leij, F. J. and M. Th. van Genuchten, 1999, A bootstrap-neural network approach to predict soil hydraulic parameters. In: Van Genuchten, M.Th., F.J. Leij, and L. Wu (Eds), Proc. Int. Workshop, Characterization and Measurements of the Hydraulic Properties of Unsaturated Porous Media, pp 1237-1250, University of California, Riverside, CA.

van Dam, J. C., J. Huygen, J. G. Wesseling, R. A. Feddes, P. Kabat, P. E. V. van Walsum, P. Groenendijk, and C. A. van Diepen, 1997, Theory of SWAT version 2.0. Simulatio of water flow, solute transport and plant growth in the Soil. Water. Air. Plant environment. Technical Doc. 45. Alterra, Wageningen, the Netherlands.

H33C-1554

Seasonal prediction for hydro-meteorological variables in the Korean Peninsula: Links with atmospheric teleconnections

SunKwon Yoon(skyoon@apcc21.org)
Climate Application Department, APEC Climate Center, 12 Centum 7-ro, Haeundae-gu Busan, 48058 Republic of Korea

Introduction

- Sea Surface Temperatures (SST) in the tropical Pacific Ocean and Indian Ocean has been reported to have experienced a change in the cycle, intensity, and genesis of El Niño
- New type of El Niño phenomenon and IOD has caused changes in the hydrometeorological patterns throughout the world
- However, quantitative studies on features of CT/WP El Niño and IOD were found to be relatively insufficient for the Korean watersheds
- Nonlinear behavior links with atmospheric teleconnections between hydrologic variables and climate indices using statistical models over the Korean Peninsula (KP)
- The ocean-related major climate factors such as the El Niño-Southern Oscillation (ENSO) and the Indian Ocean Dipole (IOD) mode in the Tropical Ocean (TO) region were used to analyze the atmospheric teleconnections by principal component analysis (PCA) and a singular spectrum analysis (SSA)
- The nonlinear lag time correlations between climate indices and hydrological variables are calculated by the Mutual Information (MI) techniques

Motivation and Data Use

Research Goal and motivation

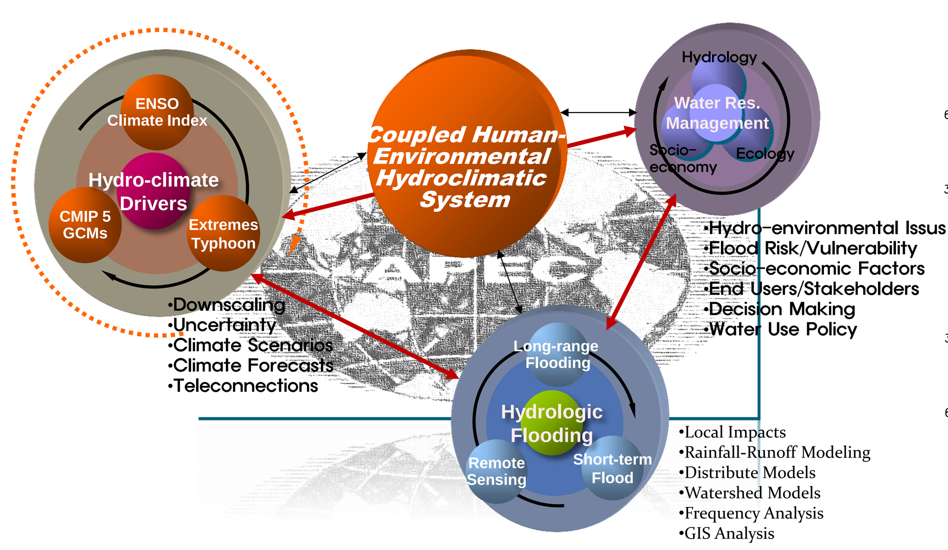

ENSO, IOD, and their Interaction

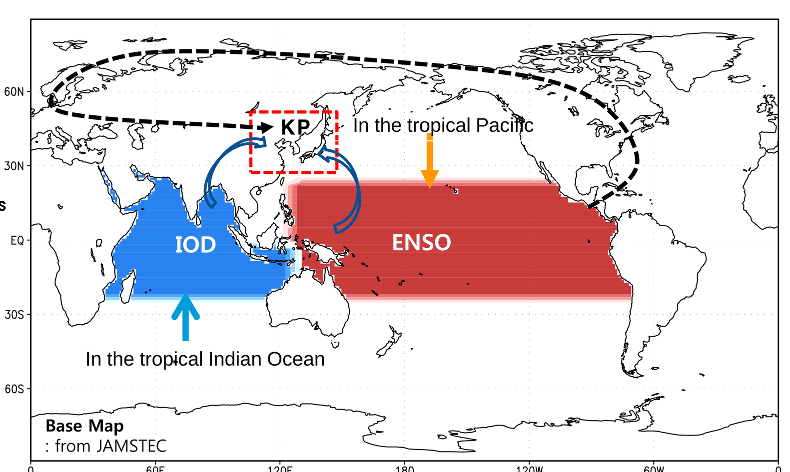

Data Source

- SST from NOAA, (URL: http://www.esrl.noaa.gov/psd/data/climateindices/list/)
- Global Precipitation data:
  - NOAA GPCP, (URL: http://www.esrl.noaa.gov/psd/cgi-bin/data/composites/printpage.pl)
  - NOAA GPCC, (URL: http://www.esrl.noaa.gov/psd/cgi-bin/data/composites/printpage.pl)
- Hydro-meteorological data:
  - Rainfall and Weather data from KMA, ASOS observed data and AWS data
  - Streamflow data from WAMIS, (URL: http://wamis.go.kr/)

Methodology

Teleconnections using Mutual Information(MI)

Flow Chart of Study

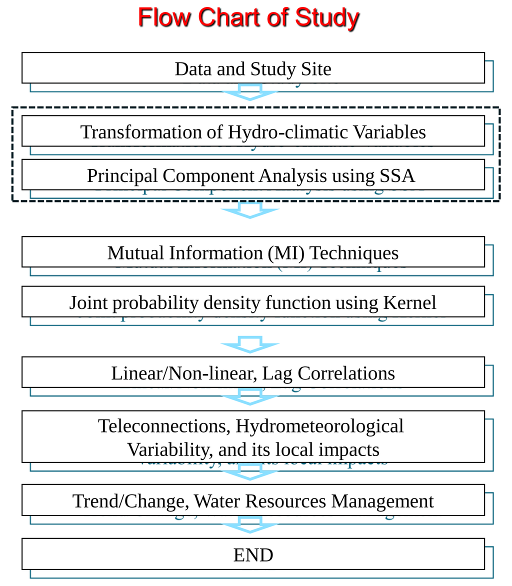

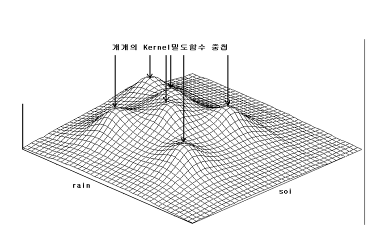

- Mutual Information(Fraser and Swinney, 1986)

$$MI_{s,q}(s_i,q_j)=\log_2\left(\frac{P_{s,q}(s_i,q_j)}{P_s(s_i)P_q(q_j)}\right)$$

- Average Mutual Information

$$I_{s,q}=\sum_{i,j}P_{s,q}(s_i,q_j)\log_2\left(\frac{P_{s,q}(s_i,q_j)}{P_s(s_i)P_q(q_j)}\right)$$

Korean Peninsula:

Non-Linear lag time corr. between Streamflow and ENSO (N_{WP})

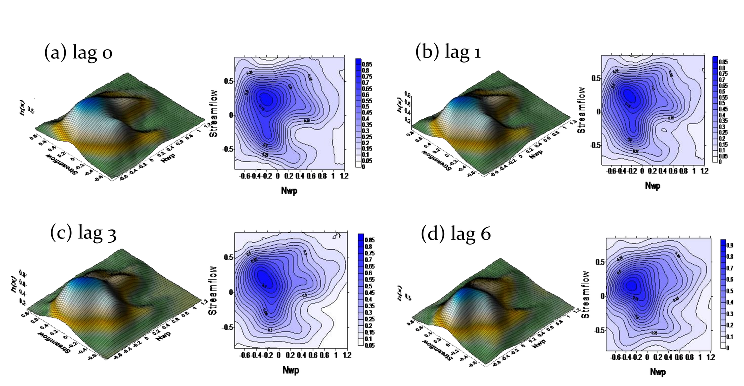

SSA and Mutual Information(MI) Process

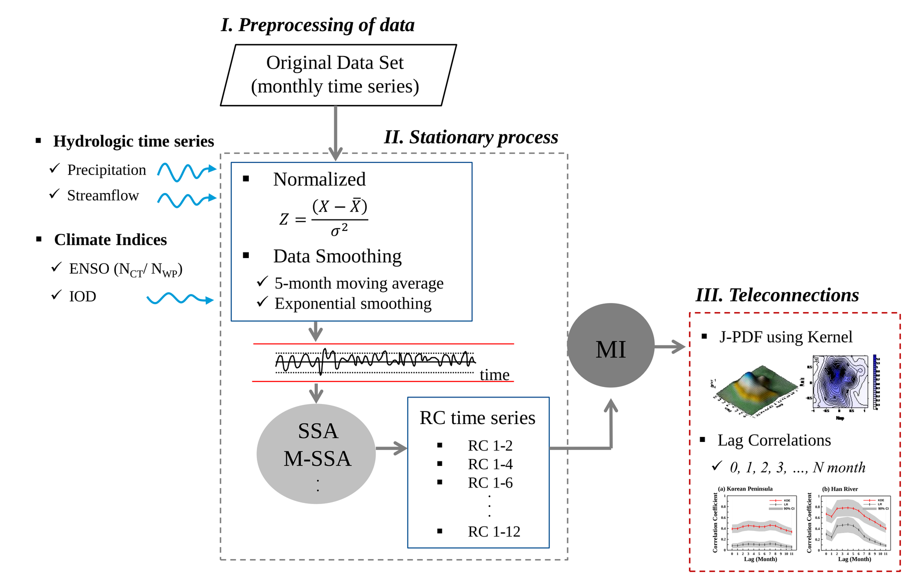

5-Major river Basin in the Korean Peninsula:

Nonlinear and linear CCs with their 90% confidence bounds among ENSO/IOD indices and Hydro-meteorological Variables

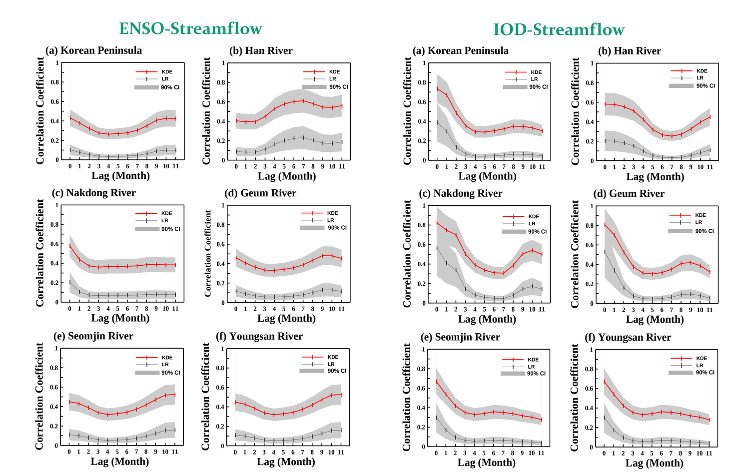

Results

Composite sea surface temperature anomalies (SSTA) of different type of ENSO and IOD

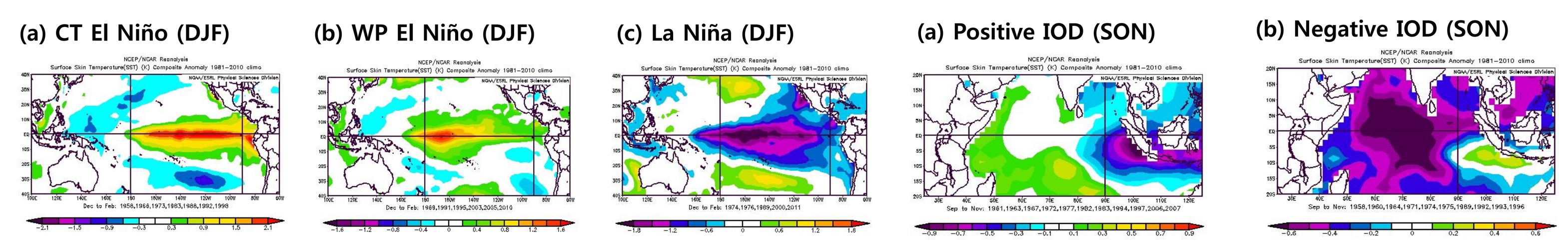

Different Type of ENSO conditions	The Strong years during 1960-2013
CT El Niño	1965/66, 1972/73, 1982/83, 1987/88, 1991/92, 1997/98
WP El Niño	1968/69, 1990/91, 1994/95, 2002/03, 2004/05, 2009/10
La Niña	1973/74, 1975/76, 1988/89, 1999/00, 2010/11

Different Type of IOD conditions	The Strong years during 1956-2013
Positive IOD	1961, 1963, 1967, 1972, 1977, 1982, 1983, 1994, 1997, 2006, 2007
Negative IOD	1958, 1960, 1964, 1971, 1974, 1975, 1989, 1992, 1993, 1996

Variability of hydro-meteorological variability during different ENSO conditions

- Rainfall variability
- Streamflow variability

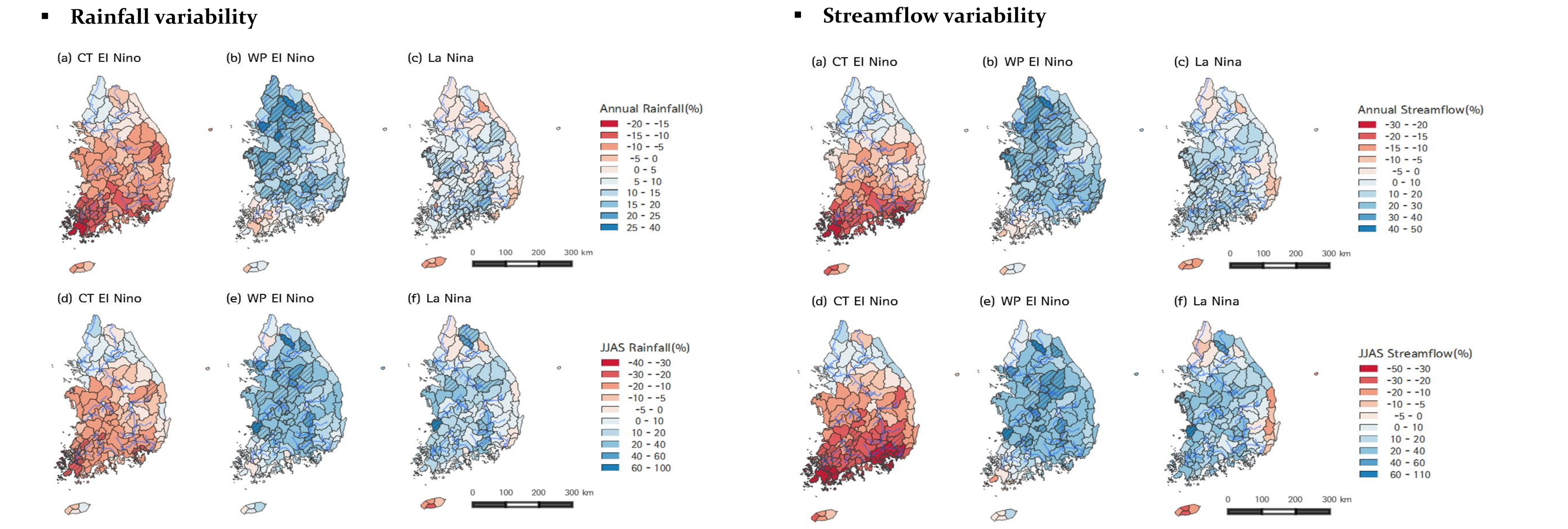

Figure 1. Composite anomalies of annual and JJAS (June to September) rainfall and streamflow during CT/WP El Niño and La Niña years. The hatched polygons indicate statistically significant changes in annual rainfall based on the 10% significance level.

Seasonal Variability of Rainfall during IOD phases

- Positive (+) IOD
- Negative (-) IOD

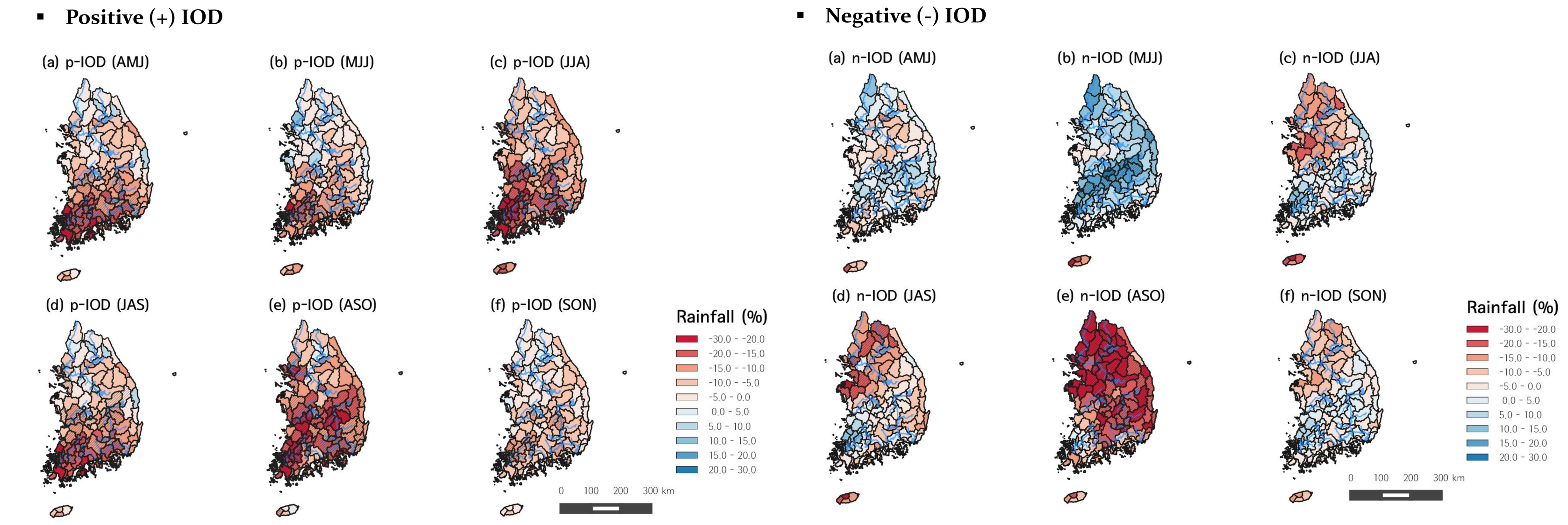

Figure 2. Composite anomalies of seasonal rainfall during positive and negative IOD years. The hatched polygons indicate statistically significant changes in rainfall based on the 10% significance level.

Seasonal Forecasting of Hydro-meteorological Variables

- Eigen vector and eigen values using PCA and SSA

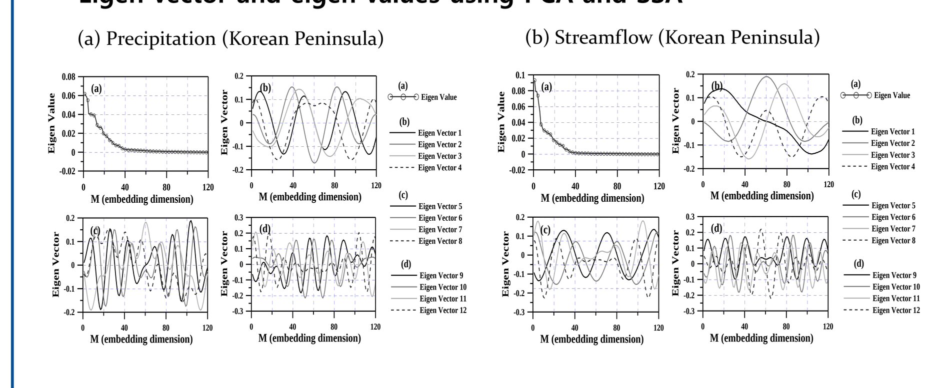

- Reconstructed components (RC)

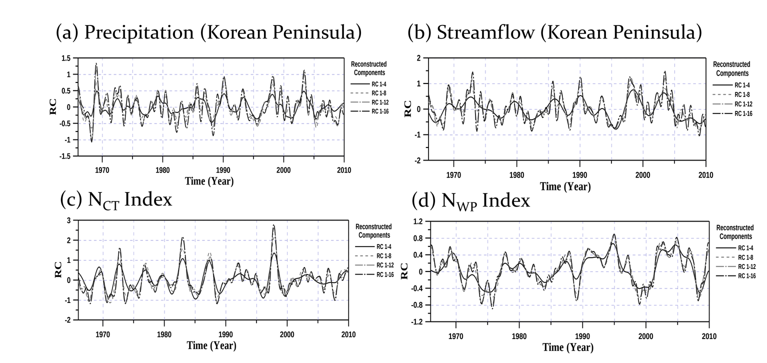

- Seasonal forecasting of rainfall over KP

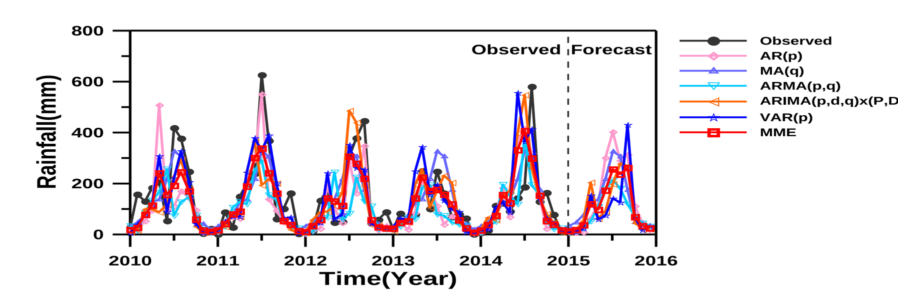

- Seasonal forecasting of ENSO in the TPO region

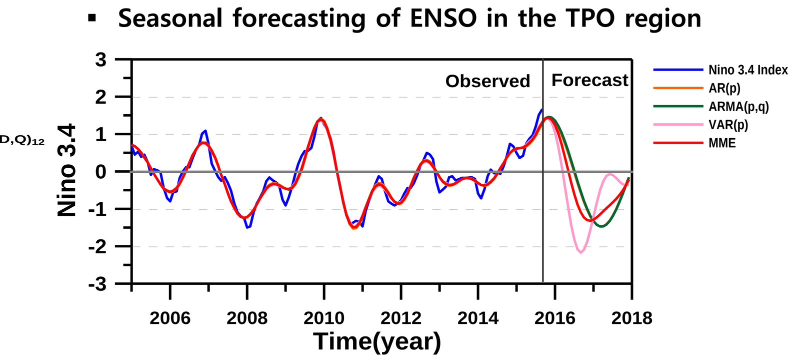

Figure 3. Scatter plot of percentage change anomaly (departures from the 1971-2000 normal) between precipitation and streamflow during JJAS season in different climate conditions of (a) ENSO, and (b) IOD modes in the 113 sub-watershed in the Korean Peninsula.

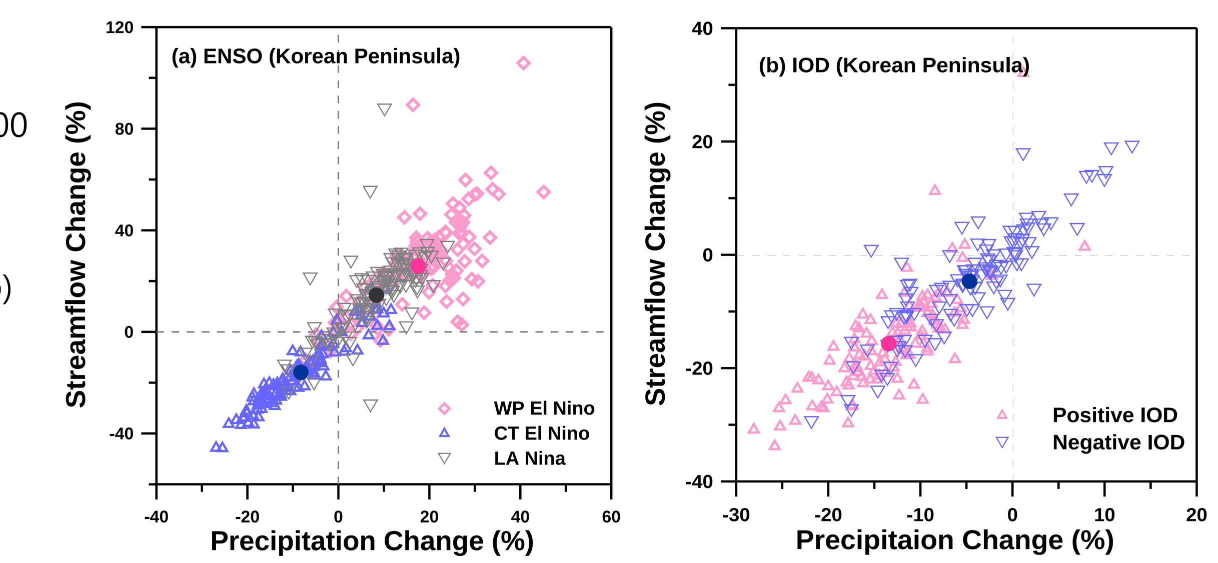

Summary

- During WP El Niño events shows substantially increasing tendency than normal years, particularly, during CT El Niño events shows significantly decreasing tendency compared to the normal years in the KP and its sub-watershed. And during La Niña years shows slightly increasing tendency and normal.
- During positive IOD events show substantially decreasing tendency than long-term normal years, and during negative IOD events show slightly below than normal tendency.
- Teleconnection based nonlinear and linear CCs are performed between climate indices and hydrologic variables using KDE and LR based on MI.
- Nonlinear CCs were higher than linear correlations, and ENOS has a few months lag time correlation and IOD has direct influence on rainfall and streamflow anomalies over the KP region
- A better understanding of the relationship between climate indices and streamflow can help policy makers prepare for possible options in river discharge pattern changes. Furthermore, these results provide useful information for water managers and end-users to support long-range water resources prediction and water-related management plan.

Reference

- Yoon, S. K., J. S. Kim, J. H. Lee, and Y. I. Moon. 2013: Hydrometeorological variability in the Korean Han River Basin and its sub-watersheds during different El Niño phases. *Stoch. Environ. Res. Risk Assess.*, **27**, 1465–1477.
- Yoon, S. K., and T. S., Lee. 2016: Investigation of hydrological variability in the Korean Peninsula with the ENSO teleconnections, Proc. IAHS, 374, 165-173, doi:10.5194/piahs-374-165-2016.